AMAS Workshop on Modelling in Biomechanics
MiB'03 – (pp.53–97) – Warsaw, April 7–11, 2003.

# Computational theories of bone modeling and remodeling

R. HUISKES

*Department of BioMedical Engineering*
*Section 'Bone and Orthopaedic Biomechanics'*
*Eindhoven University of Technology (TU/e)*
*r.huiskes@tue.nl*

## 1. Introduction

The adaptive remodeling capacities of bone are immensely important. It has long been known that bones adapt to the functional mechanical requirements to which they are exposed. Reduced mobility and lack of gravity cause osteoporosis – loss of bone mass. Excessive training increases bone mass, bones affected by trauma outgrow their maldeformities and teeth subjected to abnormal external forces migrate through the jaw bone. This principle of functional adaptation in bones has become known as 'Wolff's Law' [Wolff, 1986]. Many Orthopaedic surgical procedures are based upon its workings. These procedures have as their main objective "... to restore musculoskeletal function by creating the mechanical and biological environment in the musculoskeletal tissues which allows them to heal, adapt and maintain themselves" [Huiskes, 1996a]; Wolff's Law might be a significant factor in that goal. A notorious example of where adaptive bone remodeling may work against us is after an arthroplasty. Suddenly, the load which is normally carried by the bone alone, is now shared with the implant. The bone is stress shielded and as an effect it resorbs. Although this will not produce a clinical failure immediately, it may eventually, and certainly reduces the prospects of a revision operation. Maybe even more important is to understand the mechanical effects on bone modeling and remodeling in order to understand the causes of osteoporosis, and to find ways to prevent, or even cure it. Osteoporosis affects more than 30% of the older populations in a serious way, leading to hip, wrist and spine fractures.

Wolff's Law is not one in the sense of a quantitative, falsifiable statement in line with the tradition of the natural sciences, but rather a collection of paradigms, based on a series of observations. Instrumental in particular for the development of Wolff's theories was the work of the anatomist Meyer and the engineer Culmann, who discovered a remarkable similarity between the trabecular architecture of the proximal femur and the patterns of stress trajectories, calculated in a mathematical model, using the new theory of 'Graphic Statics', developed by Culmann. From its results grew the paradigm that bone may be a mechanically optimal structure of maximal strength and minimal weight. At this point, it is noteworthy that in our time we also have a new tool of mechanical analysis at our disposal, the Finite Element Method; immensely more powerful and precise than Graphic Statics. It stands to reason that this method is applied to re-investigate the questions posed more than a century ago [Huiskes and Hollister,1993]. The second of Wolff's paradigms, that of mechanically driven adaptive remodeling, had been discussed earlier in the writings of Roux [1881]. Roux suggested the adaptive remodeling process to be governed by a "quantitative self-regulating mechanism", nothing else "but what nowadays would be described as a biological control process," [Roesler, 1987].

If we are to predict its results in terms of bone structure quantitatively, we need to capture it in mathematical expressions. For that purpose we consider two parts of the process. One part regulates the transformation of bone loads into tissue loads, given the bone structure at any particular time. This process can conveniently be quantified in finite-element analyses [Huiskes and Hollister, 1993] The second part regulates the effects of tissue loads on bone structure, of which we know virtually nothing in quantitative terms. An approach typical for physics, designed to overcome this problem, is to start with intuitively sensible relationships, and check empirically whether they produce valid results [Huiskes, 1995a]. Such a relationship is called a remodeling model, or rule [Huiskes et al., 1987].

These models generally take the form

$$\frac{dM}{dt} = f(x,\rho)\{\sigma(x,t,\rho) - c\sigma_0(x,\rho)\},$$

where $M(x,t)$ is the bone mass in location $x$, $t$ is time, $\rho(x,t)$ is local bone density, $f$ and $c$ are weight factors, $\sigma$ is a mechanical signal (tensor or scalar), and $\sigma_0$ is a normal reference signal. The value of $\sigma - c\sigma_0$ can be construed as an error function in a local optimization process.

The formula represents the expectation that the rate of bone-mass reduction or addition is locally regulated by the difference between the mechanical signal value ($\sigma$) the tissue experiences in a particular period and the value

it is used to experience normally ($\sigma_0$); or, in other words, the latter is the target value (or reference) for the former in the remodeling process. Where the difference is positive, bone mass is locally added, where it is negative, bone is removed. The precise character of the mechanical signal is unknown, so empirical choices are to be made if the remodeling rule is to be applied. For its application FE-models are made and used in computer-simulation procedures in which the process is followed iteratively, starting from particular initial conditions – like the fixation of an implant, or alternative external loading characteristics – until no more changes in bone mass are predicted in the computations.

One could say that Wolff's Law [1892] was already based on the comparison between trabecular morphology and the results of a 'computational' analysis [Huiskes 2000]. The philosophy behind the computer simulation studies in this area is similar to those discussed above for tissue differentiation. Hart [2001] recently wrote an excellent historical overview of theories and computational models. Modern developments started with the 'theory of adaptive elasticity' for cortical bone [Cowin & Hegedus 1976], which was later used for an FEA simulation model by Hart et al. [1984]. These studies examined the adaptation of cortical form to external forces. Alternative theories were proposed and used by Huiskes et al. [1987], Mattheck et al. [1998], Prendergast & Taylor [1994] and van der Meulen et al. [1993]. Adaptation of (trabecular) bone density was simulated by several groups, using different isotropic [Beaupré et al. 1990, Carter et al. 1987, Huiskes et al. 1987, Weinans et al. 1992.a, 1992.b] or anisotropic theories [Hart & Fritton 1997, Jacobs et al. 1997, Luo et al. 1995]. All these trabecular simulation models were phenomenological in nature and simulated the outcome of coordinated osteoclastic and osteoblastic activity as either a net increase or decrease in density. A more mechanistic approach is necessary to represent the true physiology of the adaptation process, which occurs only on trabecular surfaces [Huiskes 2000]. A model to simulate local trabecular adaptation that does allow this surface mechanism to be simulated, and also includes a biological osteocyte mechanosensory and signaling function, was developed by Mullender & Huiskes [1995]. A model that also includes separate descriptions of osteoclastic resorption and osteoblastic formation, enabling simulation of mechanobiologically modulated growth, adaptation and maintenance (remodeling) was published recently [Huiskes et al. 2000, Ruimerman et al. 2001]. Adachi et al. [2001] proposed a phenomenological adaptation model for the trabecular structure using nonuniformity of the local surface stress distribution as the regulatory feedback signal. The models incorporating trabecular morphology have been used only to study adaptation in small cubes of bone. Analyses of whole bone FEA models with refinement down to the trabecular level are

feasible now [van Rietbergen et al. 1999]. However, there is not enough computer capacity yet to use those in iterative simulations to study trabecular adaptation based on a (mechanistic) cell modulation scheme. Future models will need to include both natural boundary conditions at external bone surfaces and refined trabecular architecture.

## 2. Regulation of bone density

With increasing computer capacity, computer simulation of bone adaptation in whole bones became in reach in the late 1980's. The early models, based on finite element analysis (FEA), calculated mechanical signals within the bone that were assumed to initiate changes in density or material properties, for which process numerical formulations of adaptive bone remodeling theories were applied. The models were empirical and related mechanical signals, like stress or strain, to bone adaptation, without direct consideration of the underlying cel-biological mechanisms. They were applied to complete bones and simulated adaptation of bone tissue on a macroscopic level. In the work of Fyhrie and Carter (1986a) the bone tissue was considered as a continuum, characterized by particular apparent density value distributions. The bone was assumed to be a self-optimizing material with the objective to adapt its apparent density $\rho$ to an 'effective stress' $\sigma_{\text{eff}}$. Based on strength or strain optimization criteria they derived

$$\rho = A\sigma_{\text{eff}}^{\alpha}, \tag{2.1}$$

where $A$ and $\alpha$ are constants, and the effective stress is determined from either a failure or an elastic energy criterion. In later publications (Carter 1987; Fyhrie & Carter, 1986) they assumed $\alpha = 0.5$ and for the effective stress, and postulated

$$\sigma_{\text{eff}}^{\alpha} = 2EU, \tag{2.2}$$

where $E$ is the apparent elastic modulus and $U$ the apparent strain energy density (SED). By assuming a modulus-density relation of $E = c\rho^3$ (Carter & Hayes, 1977), with $c$ a constant, the optimization function transforms to

$$\rho = c'U, \tag{2.3}$$

where $c'$ is a constant. Applying this optimization criterion made it possible to predict a density distribution of the proximal femur assumed optimal (Carter et al., 1987; Fyhrie and Carter, 1986b). To test the theory they visually compared the resulting density patterns to those in radiograms of a real femur, and observed some similarity in it.

### Internal and external remodeling

Frost (1964, 1987) suggested that internal and external remodeling[1)] should be distinguished. Internal remodeling is the adaptation of the density of bone tissue, while external or surface remodeling is the apposition or removal of bone tissue on the bone surface. The two forms were actually separated by Cowin and associates and by Huiskes and coworkers. Cowin et al. (1981, 1985) used the strain tensor as the mechanical signal to be the driving factor of bone adaptation, and assumed a quadratic relationship between strain and the rate of adaptation (Firoozbakhsh and Cowin, 1981). Huiskes and coworkers (1987) used the strain energy density (SED) $U$ [J/mm$^3$] as the signal that controls remodeling of the bone, with

$$U = \frac{1}{2}\varepsilon_{ij}\sigma_{ij}. \tag{2.4}$$

The relation between adaptive rate and SED was linear. For external surface remodeling the bone can either add or remove material, according to

$$\frac{dX}{dt} = C_{\mathrm{x}}(U - U_{\mathrm{n}}), \tag{2.5}$$

where $\frac{dX}{dt}$ is the rate of bone growth perpendicular to the surface, $U$ the SED, $U_{\mathrm{n}}$ a homeostatic SED, and $C_{\mathrm{x}}$ a proportionality constant. For internal remodeling the bone could adapt its density value. Assuming that the elastic modulus relates to the apparent density one can write

$$\frac{dE}{dt} = C_{\mathrm{e}}(U - U_{\mathrm{n}}), \tag{2.6}$$

where $E$ [MPa] is the local elastic modulus, and $C_{\mathrm{e}}$ a proportionality constant.

Carter (1984) suggested that bone is 'lazy' in terms of reacting to mechanical signals. The concept of a so-called 'lazy zone', meaning that there are thresholds to be exceeded before bone adaptation could occur (Fig. 1), were incorporated by Huiskes et al. (1987). The SED was compared to a homeostatic one, $U_{\mathrm{h}}$. For $U > (1+s)U_{\mathrm{h}}$ or $U < (1-s)U_{\mathrm{h}}$ adaptive activity is initiated, whereby $s$ is the threshold level that marks the borders of the lazy zone. The remodeling rule transforms to a new set of equations for internal remodeling

[1)] Although 'modeling' and 'remodeling' of bone were clearly defined by Frost (1964) as change in shape (as in growth) and the subsequent localized resorption and formation of bone, the term 'remodeling' is often used in biomechanics as if to mean 'adaptation'. In fact, 'modeling' is closer to adaptation than 'remodeling'.

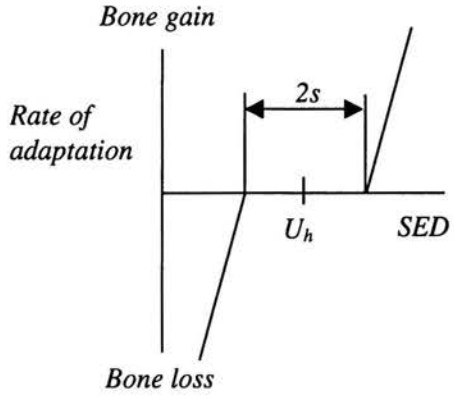


FIGURE 1. The assumed local adaptation as a function of the strain energy density (SED). There is no adaptive response in the "lazy zone".

$$\begin{cases} \dfrac{dE}{dt} = C_e(U - (1+s)U_n) & \text{for} \quad U > (1+s)U_n, \\ 0 & \text{for} \quad (1-s)U \le U \le (1+s)U_n, \\ C_e(U - (1+s)U_n) & \text{for} \quad U < (1-s)U_n \end{cases} \tag{2.7}$$

and a similar set of equations for external remodeling.

This theory was applied to predict the density distribution in the normal proximal femur. Starting from an initial uniform density distribution the simulation produced a configuration that was similar to the one obtained by Fyhrie and Carter (1986b), showing some similarity to the natural density distribution in the femur. The theory was also applied to predict cortical adaptation after hip-prosthetic implantation in a geometrically idealized model (Huiskes et al., 1987). The bone was represented as a hollow cylinder in which a cylindrical stem was placed and the effects of "stress shielding" due to load transfer through the stem could be predicted. The results illustrated the potential applicability of computer simulations for peri-prosthetic bone adaptation and encouraged further investigation. Later the theory was successfully applied to evaluate bone adaptation in a realistic 3-dimensional femur model after implantation of prostheses. Three-dimensional finite element models were constructed from an experimental animal configuration, in which smooth press fitted stems were applied. The adaptive remodeling procedure was integrated with the model and predicted similar amounts of proximal bone loss and distal bone densification as found in animal experi-

ments (Rietbergen et al., 1993; Weinans et al., 1993). The prosthetic stress-shielding theory was also validated relative to post-mortem patient series (Kerner et al., 1999.)

### Discontinuous end configurations

In the remodeling rules discussed in the previous section bone adapts towards reference states of deformation caused by single loads. To incorporate variable loading, a stimulus $S$ was defined that took account of individual loading configurations by averaging their individual contributions (Carter et al., 1989), as

$$S = \frac{1}{n}\frac{1}{\rho}\sum_{i=1}^{n} U_i, \tag{2.8}$$

here $U_i$ is the SED value for loading case $i, n$ the total number of loading cases and $\rho$ the apparent density. In order to estimate the actual SED values in the trabeculae the remodeling signal was approximated by $U/\rho$ as the strain energy per unit of bone mass (Carter et al., 1989). In 1992, Weinans et al. applied this theory to a two dimensional finite element model of a proximal femur. Bone was represented as a continuum, capable of adapting its apparent density due to mechanical stimulation. The stimulus value $S$ was measured per element, and the apparent density $\rho$ was adapted per element according to:

$$\frac{d\rho}{dt} = B(S - k) \tag{2.9}$$

with $B$ and $k$ constants and $S$ the stimulus value in the element. This theory produced density distributions that showed good resemblance with those in a real proximal femur. However, only if these distributions were locally averaged from discontinuous density patterns in the femoral head, where the trabecular bone is located (Fig. 2). In fact, the underlying patchwork of either full or empty elements is inadmissible relative to the mathematical basis of FEA. However, Weinans et al. (1992a) also showed that it is in the nature of the differential equations used to mathematically describe the adaptive remodeling process that the simulation produces discontinuous end configurations, a phenomenon called "checker boarding". Using an analytical two-unit model they showed that the differential equations have an unstable uniform solution and that the slightest non-uniformity causes stress shielding by the stiffer elements. Hence, in the ongoing process the stiffer elements will even become stiffer, while the others loose density, until they are virtually empty, so that a "checkerboard" results (Fig. 2). This phenomenon is the result of capturing both sensation of the local mechanical stimulus and actual

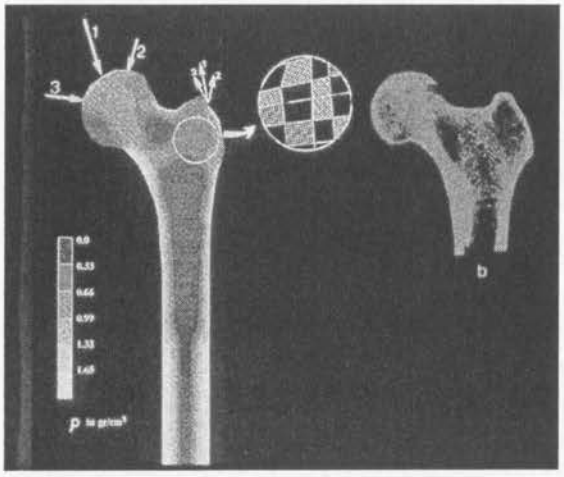


FIGURE 2. Applied to a femur model and starting from a uniform density distribution the simulation model of Weinans et al. (1992) produced density distributions (a), that show some similarity to the density distribution in a real femur (b).

adaptation of bone mass in that same location in one equation, which make the elements—which are artifacts for biology—'work for themselves'.

## The biology of bone development and growth[2)]

Bones provide mechanical strength to the body; they protect organs like the heart, the lungs, and the brains against trauma; they produce blood cells from bone marrow; and they serve as a calcium reservoir. Morphologically, two types of bone are present in the skeleton, cortical bone, which is dense and compact, and trabecular bone, which is porous, due to its structure of rods and plates. The latter is found predominantly in vertebral bodies and in the distal ends of long bones.

During embryonic development of long bones, cartilaginous tissue develops into bone tissue (Fig. 3).

This endochondral ossification process passes the subsequent stages of chondrocyte proliferation, chondrocyte hypertrophy (Fig. 3B), which is primarily achieved by accumulation of water [Buckwalter et al., 1986; Pauwels, 1980], and mineralization of the cartilage matrix (Fig. 3C). The mineralization process starts in the primary ossification center, in the middle of the rudiment, extends towards the periphery and subsequently towards the distal ends of the bone. Matrix vesicles play an important role in the initiation

[2)] Adapted from Tanck & Huiskes, 2003.

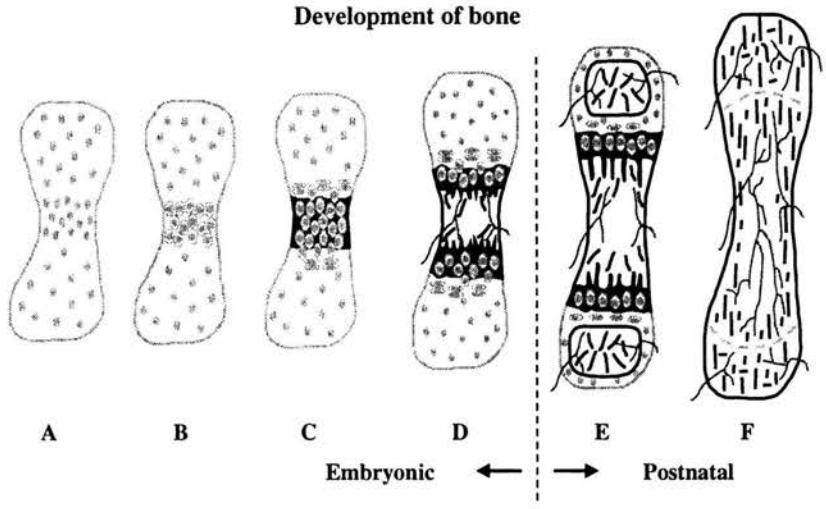


FIGURE 3. Schematic illustration of the development of long bones from embryonic to mature (figures not to scale). A) Cartilaginous rudiment; B) Chondrocytes in the center swell; C) Cartilage mineralization occurs around hypertrophic chondrocytes, proliferating, flattened cells develop; D) Blood vessels penetrate the tissue, mineralized cartilage is resorbed, bone formation takes place, and longitudinal growth commences; E) Secondary ossification centers develop and growth plates remain in between; F) The bone is mature, the growth plates are closed.

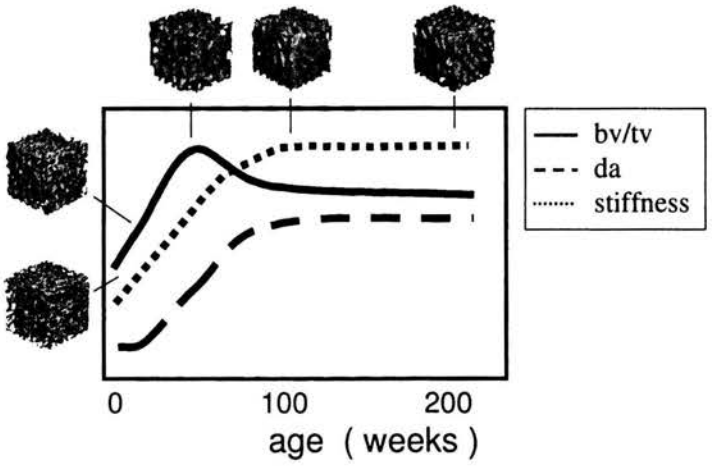


FIGURE 4. Development at large of bone volume fraction (bv/tv), degree of anisotropy (da), and stifness of trabecular pig bone during growth.The change in trabecular structure of pig vertebrae during growth is shown as well.

of mineral deposition [Kirsch et al., 1997], but the actual mineralization process is a physical one, occurring in the extracellular matrix by deposition of a calcium phosphate. Mineralization proceeds very fast. In embryonic metatarsals of the mouse, for example, about one-fourth of the metatarsal is mineralized within one day (Fig. 4).

[Burger et al., 1992; Haaijman et al., 1997; Tankck et al., 2000; van Loon et al., 1995]. Mineralization always occurs around hypertrophic chondrocytes. Shortly after the matrix is mineralized these cells die by apoptosis [Bronckers et al., 1996]. Blood vessels penetrate the tissue (Fig. 3D), the mineralized cartilage is resorbed by osteoclasts, and bone tissue is formed by osteoblasts on remnants of mineralized cartilage. At the distal ends of the bone, the secondary ossification centers develop, in which the same cascade of processes takes place (Fig. 3E). These centers create the trabecular bone of the epiphyses. Between the primary and secondary ossification centers, cartilaginous growth plates remain, in which the endochondral ossification process continues (Fig. 3D and Fig. 3E). In this way, the length of bones increases. During growth to maturity, cell proliferation, matrix production, and cell swelling determine the longitudinal growth rate [Hunziker et al., 1989].

In addition to longitudinal growth, the growth plate continuously produces new bone trabeculae in the metaphysis, oriented in the direction of the marrow cavity. Eventually, these trabeculae are remodeled to optimally withstand the forces on the bone (Wolff's Law). At maturity, chondrocyte proliferation stops and the growth plates are closed (Fig. 3F). All cartilage is then replaced by bone tissue, except at the joint surfaces, where a layer of articular cartilage remains present.

New bone is formed from the growth plate towards the marrow cavity (Fig. 3E). The bone tissue on the remnants grows and subsequently fuses into a trabecular structure. During this process, bone resorption is hardly present and the trabecular structure consists of woven bone. Later, the woven bone is replaced by lamellar trabecular bone, where bone resorption as well as bone formation take place. When the trabecular architecture is formed, it is continuously remodeled. Frost [Frost, 1987] defined growth and development of the trabecular structure and later morphological adaptation- as 'modeling', whereas the stage of dynamic morphological equilibrium of the trabecular architecture (metabolic homeostasis), was defined as 'remodeling'. The dynamic capacity of bone metabolism has several advantages, like the competence to repair itself, but also the ability to adapt to environmental changes. If the mechanical load increases by, for instance, increased physical activity, then bone mass increases [Bailey et al., 1999]. If, on the other hand, load is decreased by bed rest or immobilization, this will lead to decreased bone mass [Leblanc et al., 1995]. Not only bone mass, but also bone architec-

ture adapts to external loads. In the adult stage, the trabeculae are aligned to the principal stress directions, as Wolff described it [1892]. In this way, trabecular bone is believed to be adapted to the typical external loads of daily living in both density and architecture.

At maturity, trabecular bone mass and architecture are adapted to the typical external loads of daily living. Little quantitative data is available on the development of architecture and mechanical adaptation in juvenile trabecular bone. Using radiographs and digital imaging, Korstjens et al. [1995] analyzed the two-dimensional trabecular patterns of the distal radius in children, aged $4-14$ years. Their study showed that the refined trabecular patterns of young children had coarsened in the older ones. Nafei et al. [2000.a, 2000.b] analyzed trabecular bone in epiphyseal proximal tibiae of immature and mature sheep. Using mechanical tests and serial sectioning, they found that architectural and mechanical properties changed significantly with skeletal maturity. A study in rats showed that the highest bone formation rates were present directly after birth [Sontag, 1992]. From there on, the formation rates decreased continuously with increasing age in both epiphysis and metaphysis, whereby formation rates were higher than resorption rates during the first 150 days of age [Sontag, 1992]. The recent development of microcomputer tomography (micro-CT) has made it possible to analyze the three-dimensional (3D) architecture of trabecular bone accurately [Feldkamp et al., 1989]. This technique has been widely used to study adult cancellous bone and to investigate the effects of aging [Ciarelli et al., 2000].

Using micro-CT, we investigated the development of the trabecular structure during growth in pigs [Tanck et al., 2001]. Pigs between 6 and 230 weeks of age, and between 12 and 212 kg of body weight were used (Table 1). During

TABLE 1. Age versus average body weight of the pigs ($N = 2$ per age group).

| age (weeks) | average body weight (kg) |
|---|---|
| 6 | 12 |
| 23 | 60 |
| 56 | 170 |
| 104 | 212 |
| 230 | 180 |

growth, body weight, hence load, increases gradually, which implies that density and architecture would change as well. As an increase in trabecular density due to increased loading would only have to involve bone formation, but the adaptation of trabecular architecture must involve both formation and resorption, we hypothesized that there is a time lag between these processes

during the development. To test this hypothesis, three-dimensional morphological and mechanical parameters of trabecular bone samples from the vertebra and proximal tibia were studied using micro-CT and micro-FEA [Tanck et al., 2001].

The results of the micro-CT showed clear differences in trabecular structure with age (Fig. 4). For the youngest bones, the structure was refined whereas in older bones it had developed into a much coarser trabecular structure. The three-dimensional morphological parameters showed that the bone volume fraction (BV/TV) increased rapidly in the initial growth phase, whereas the morphological anisotropy started increasing somewhat later during the development (Fig. 4). In addition, the maximal value of BV/TV was reached earlier in time than the maximal value of anisotropy. The development of stiffness, resulting from the micro-FEA calculations, could be explained by the combined development of volume fraction and anisotropy (Fig. 4). As stiffness and strength are highly correlated [Keaveny et al. 1994], trabecular bone also becomes stronger during growth. Interestingly, BV/TV and total body weight did not exactly follow the same trend; while total body weight reached a maximum at 104 weeks of age (Table 1), BV/TV reached its maximum at 56 weeks of age (Fig. 4). Adaptation of the trabecular architecture to the weight increase between 6 and 56 weeks of age could be explained by the increase in BV/TV. Between 56 and 104 weeks of age, adaptation of the trabecular architecture to the weight increase could be explained by the increase in anisotropy, i.e. the trabeculae aligned to the primary loading direction. By increasing the anisotropy and decreasing, or stabilizing, the trabecular density, the trabecular structure becomes more efficient to resist load in the primary loading direction. We concluded that the hypothesis was supported by the time lag between the increase in trabecular density and the adaptation of the trabecular architecture [Tanck et al. 2001].

In order to be adapted to external loads, in mass and structure, bone requires a load sensorial capacity in the form of 'mechanosensors'. This function can be located in the bone matrix itself, or in the bone cells. Potential strain-mechanosensory mechanisms in the bone matrix are piezoelectricity and streaming potentials [Konikoff et al., 1975; Pienkowski et al., 1983], but presently the mechanosensor function is thought to reside in bone cells. The permanent cells in bone are osteocytes and lining cells. Osteoblasts and osteoclasts are attracted to the bone, from the marrow and responsible for bone formation and resorption, respectively. In other words, they are able to change bone mass and bone architecture. They both are attracted to, and active at the bone surface. Some of the osteoblasts become osteocytes when they are encapsulated by the bone matrix that they produce. Others cover the new bone matrix as lining cells. Osteocytes are matured osteoblasts, sur-

rounded by calcified bone. The osteocytes in the bone matrix are regularly distributed throughout the bone. They are connected to each other and to the lining cells at the bone surface by their canalicular processes. Through this cannalicular network, nutrients can be transported from the lining cells to the osteocytes and vice versa. In addition, biochemical products can be transported between the osteocytes, and from osteocytes to lining cells. With these properties, osteocytes would be excellent candidates to serve as the mechanosensors of bone [Klein Nulend et al., 1986]. Many experiments have been performed and several theories have been developed to test this hypothesis. Mechanical strain is an important regulator of bone homeostasis, but the mechanism whereby bone tissue detects the strain, and how this results in anabolic or catabolic responses, is only partially understood [Burger et al., 1998]. Skerry et al. [1989] showed an increased enzyme activity of osteocytes following bone loading in vivo. This increase was proportional to the strain magnitude in the bone tissue. Weinbaum et al. [1994] proposed that the in vivo strains in the calcified matrix could be sensed by the osteocytes through small fluid shear stresses. Bone fluid flows through the bone pores, which are filled with a proteoglycan matrix [Weinbaum et al., 1994; Cowin et al., 1995]. The combination of bone fluid and matrix is thought to function as a gel, which acts on the membranes of the osteocytic processes [Weinbaum et al., 1994; Cowin, 1999]. The intracellular actin cytoskeleton could also amplify the deformation of osteocytes by fluid drag forces [You et al., 2001]. Klein-Nulend et al. [1995] studied the effect of pulsating fluid flow and intermittent hydrostatic pressure on isolated osteocytes, osteoblasts, and periosteal fibroblasts. Pulsating fluid flow increased the Prostaglandin E2 production of the osteocytes, whereas osteoblasts and fibroblasts did not react to the applied flow. The effects of hydrostatic pressure were less pronounced; osteocytes as well as osteoblasts reacted to hydrostatic pressure, though the production of prostaglandin was less, relative to the reaction of osteocytes to fluid flow. It was concluded that osteocytes were the most mechanosensitive cells in bone, reacting most profoundly to pulsating fluid flow [Klein Nulend et al., 1995]. Jacobs et al. [1998] tested the effect of oscillating and pulsing fluid flows on bone cells with 0.5, 1.0, and 2.0 Hz frequencies. They showed that oscillating fluid flow and pulsing flow were stimulatory to bone cells and that dynamic flows became less stimulatory with increasing frequency. Oscillating flow was less stimulatory than pulsing flow, suggesting that different cellular mechanisms could be involved in these flow modalities [Jacobs et al., 1998]. The effects of load-induced fluid flow were observed and quantified after four-point bending loads on rat tibiae in vivo by Knothe-Tate et al. [2000]. The transport of small and large molecular-mass tracers was enhanced by mechanical loading, whereby the small molecules showed the fastest transport

through the tissue. These results indicated that mechanical loading is able to modulate the distribution and concentration of bone fluid tracers within the tissue. In summary, strain induced fluid flow is a prominent candidate for the primary stimulus for osteocyte mechanosensation.

## 3. A regulatory model for trabecular morphogenesis and adaptation[3)]

Roux [1881] suggested that formation and functional adaptation of trabecular architecture in bone is regulated locally by cells, governed by mechanical stimuli, in a self–organizational process. It was not stated in those terms then, but this is clearly what he was on to. Nothing else "but what nowadays would be described as a biological control process" [Roesler, 1987]. Although this sounds quite reasonable in our time, in which regulatory processes and control theory are well known, it hardly moved the scientific community in bone biology. Biochemists and cell-biologists have considered biological processes in bone, but the mechanical vector was somehow lost. Pauwels [1965] knew Roux's theories well and investigated the nature of tissue loading patterns, and how they could promote particular kinds of tissues being formed; a work that was extended later by Carter [1987]. But it was probably Frost [1987] who stepped in Roux's footprints in the most direct sense. In his conceptual 'mechanostat' theory, local strains are assumed to regulate bone mass, like the local temperature in a room regulates the heater, through a thermostat. The BMU's – 'basic multicellular units' of osteoblasts and osteoclasts – are supposed to maintain local bone mass, controlled by a 'mechanical feedback loop', and a 'set point', which is the quantitative setting for the balance between strain and bone mass. Frost pointed out that this control process is purely biological in its components, be it governed by mechanical loads. His theories have contributed greatly to the awareness of mechanical factors in the regulation of bone modeling, remodeling and repair in orthopaedics and bone biology. But although many a biological reality can be brought to its support, it is still a qualitative theoretical construction of several hypotheses. Using large-scale computer simulation, however, these kinds of proposals can now also be tested in an integral quantitative sense; an example of which is discussed here.

The regulatory model we investigated is shown schematically in Fig. 5, [Mullender et al., 1994; Mullender and Huiskes, 1995]. We assumed osteocytes to be the mechanosensors; this is where the 'mechanostat' is assumed to be located. According to the literature this assumption seems reasonable [Skerry

[3)] Adapted from Huiskes, 2000.

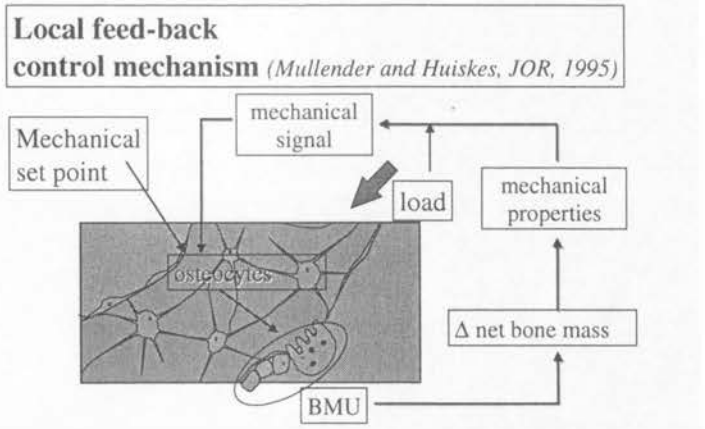


FIGURE 5. Schematic representation of the regulatory process assumed for the computer-simulation of bone remodeling. Load on bone is distributed by the trabecular architecture, and locally sensed by osteocytes (the remodeling signal). Based on the 'set-point', a reference value for the typical loading rate, the osteocytes send a biochemical messenger (the remodeling stimulus) to the bone surface, which regulates net bone resorption or formation by Basic Multicellular Units of osteoclasts and osteoblasts. Both increases and decreases in local bone mass affect the trabecular loading patterns, hence also the signal value. Thus, the effect of stimulation is fed back to the cause of stimulation, which makes the adaptation process continue until equilibrium is reached.

et al., 1989; Cowin et al., 1991; Lanyon, 1993; Klein Nulend et al., 1995]. It is uncertain to which mechanical signal these cells would react; stress, strain or a combination thereof, but we postulate that it is the elastic energy stored locally in the bone matrix upon external loading, the strain-energy density (SED) [Carter et al., 1987; Huiskes, 1997]. It is known that static loads have no effects on bone mass; experimental information makes it plausible that amplitude, rate, frequency and duration of loading are all important for bone metabolism [Turner, 1998]. To account for this, we focus on the rate of change of the SED as a function of time.[4)] This introduces two different time frames in the regulatory process, the one of load application, on the order of seconds, and the one of remodeling, on the order of days [Luo et al., 1995]. The remodeling time is denoted by $t$ and the load-application time is denoted by $\underline{t}$; hence the periodic external load causes a time-dependent SED variation $S(\underline{t})$ (MJ/m$^3$) in the bone matrix, with a rate of $R(\underline{t})$ (MJ/m$^3$s). We now

[4)]In the original publication [Mullender and Huiskes, 1995], the remodeling signal was assumed to be the (static) value of the SED. It was found, however, that the results obtained are equivalent with the typical SED-rate from a sinusoidal external load, with a frequency of about 0.25 Hz. This is explained in the next section.

assume that the osteocytes react to a typical SED-rate in a recent loading history; hence, this variable we consider as the mechanical remodeling signal. This typical SED-rate $R_t$ is variable not in the load-application time frame, but only in the remodeling time frame; hence $R_t = R_t(t)$ (MJ/m$^3$s). During the iterative computer-simulation procedure the value of $R_t$ is compared continuously to a reference rate $k$ (MPa/sec) which is the value the osteocytes are supposed to be used to in homeostasis. Based on the difference, the osteocytes, through their network, provide a stimulus to the BMU's at the trabecular surface to either increase or reduce net local bone mass, according to

$$F(\underline{x}, t) = \sum_{i=1}^{N} f_i(\underline{x})(R_{ti(t)} - k).$$

In this regulatory scheme, evaluating the remodeling stimulus $F$ at location $\underline{x}$ of the bone surface, $R_{ti}$ is the signal value (the typical SED-rate) in osteocyte $i$, $N$ is the total number of osteocytes and $k$ the reference signal value. The $\sum$ symbol in the formula represents summation of the remodeling stimuli over all osteocytes. The amount of stimulus a BMU receives from a particular osteocyte depends on its distance away from it. This is taken into account by the exponential decay function $f_i$ (Fig. 6). This function has a characteristic

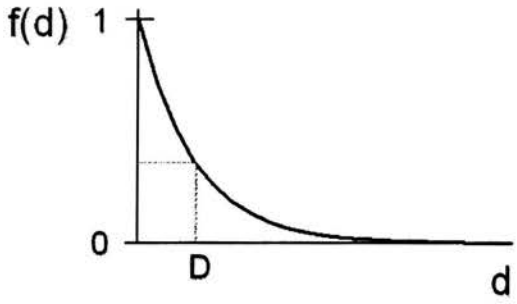


FIGURE 6. The remodeling stimulus, sent to the bone surface by an osteocyte, as an effect of its loading signal, is assumed to decay exponentially over distance. At a distance $D(m)$ away the stimulus is reduced in intensity to 37%. It turns out that the parameter $D$ controls average trabecular thickness, for a given external force.

parameter $D$, which is the distance at which the value of an osteocyte signal is assumed to be reduced to 37 percent of the value sent. As a net effect of the total stimulus received by BMU's at location $\underline{x}$ we consider the development

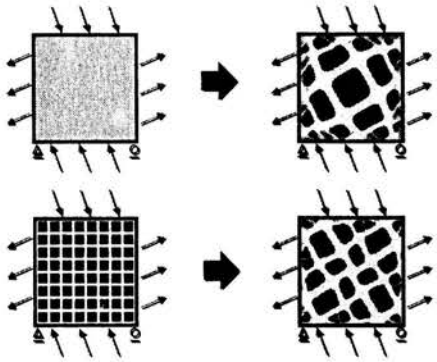

FIGURE 7. After the application of loads to a homogeneous field, the regulatory scheme predicts the morphogenesis of trabecular architecture. The struts are oriented according to the external load directions. Starting from an arbitrary lattice structure, not aligned with the external load, an architecture is created of which both trabecular thickness and orientation are adapted to the external load [Mullender and Huiskes, 1995].

of the local degree of bone mineralization $m(\underline{x}, t)$

$$\frac{dm(\underline{x}, t)}{dt} = \tau F(\underline{x}, t) \quad \text{with} \quad 0 < m(\underline{x}, t) \leq 1,$$

where $\tau$ is a time constant.

The input to this regulatory model comprises the directions, magnitudes and frequencies of the external loads applied to the volume of bone studied, and its output is architecture, represented by a density pattern. Its physiological parameters are the homeostatic SED-rate $k$, the osteocyte density (derived from their total number $N$ and the volume considered), the exponential osteocyte-influence function (characterized by the distance parameter $D$), and the constant $\tau$ (two other constants, not discussed here, represent the relationship between tissue mineral density and its elastic properties; Mullender and Huiskes, 1995). When we applied this regulatory scheme to a 2-D FE model of a square plate, subjected to a sinusoidal external stress profile of 4 MPa peak value at 0,25 Hz (see next section), using realistic values for the parameters [Mullender and Huiskes, 1995], we see the emergence of a trabecular architecture (Fig. 7). The morphology and dimensions of the trabeculae have a realistic appearance, with an orientation loosely in accordance with that of the (external) stresses. When we changed the orientation of the external stresses, the trabecular architecture adapted accordingly.

Although the regulatory model proposed was meant to be mechanistic (or physiological) and not phenomenological, as all parameters and variables used are measurable in principle, its validity as such is unknown. Although

there are strong indications that osteocytes, and their network, are involved in mechano-sensation and transduction, the lining cells may play important roles as well [Mullender and Huiskes, 1997]. And while it is certain that BMU's play the role of remodeling effector units, the relationship with the model parameters selected is uncertain. SED-rate as a remodeling signal is only a choice; it could be other mechanical variables as well. The threshold SED-rate, the 'set-point', a necessary feature to make the model work, could in reality be variable. The separate roles of osteoclasts and osteoblasts are not considered in the model, as only net remodeling (actually 'modeling') is described. Although BMU net activity was assumed to be proportional to the stimulus, the process might also be driven by an on-off principle. These are just a few of the uncertainties.

Yet, what the model predicts is surprisingly realistic [Huiskes and Mullender, 1997]. In addition to the morphogenetic and adaptive predictions above, it was also shown that the model, applied to a 3-D representation of bone, predicts the emergence of trabecular plates, instead of struts, in regions of high shear stress [van Rietbergen et al., 1995]. It predicts the disappearance of struts in cases of disuse, and the fact that these will not re-appear, as illustrated in Fig. D4 [Mullender et al., 1998]. It predicts the relationship between osteocyte viability and effectiveness of the remodeling process [Mullender et al., 1996a]. It predicts the uniformity in average trabecular thickness for vertebrates in general [Mullender et al., 1996b].

It's too early to judge the validity of the model proposed, as other assumptions might lead to similar results. But what we have in fact accomplished is to show how the paradigm of Roux and the regulatory proposals of Frost can be captured with a very simple regulatory scheme, governed by a limited number of physiological parameters. We don't know if it actually works like this or how the cells would in fact biologically engineer such a control mechanism. But we do know that it could work like this, from a quantitative regulatory point of view. Roux may have been right. And if so, we could learn a lot more about bone when following in his footsteps.

## 4. Validation objectives

A model is a reduction from a complex reality and can only be used to investigate those phenomena that are indeed captured by it. The model described above, for example, can not be used to predict how calcium deficiency would affect trabecular architecture. It is simply assumed that the amount of calcium required for the regulatory process to function normally is present. A model is invalid outside its scope. Inside its scope we can consider its numerical validity, its predictive validity and its mechanistic validity.

Numerical validity implies that the algorithm used does not produce artefacts. Sources of such artefacts in this particular case may be inadequate refinement of mesh densities or iteration-time steps. A potential problem in the above example is that when the element-mesh size is taken too large relative to the osteocyte-influence distance (the parameter $D$), the algorithm produces checker-board density patterns and the solution becomes mesh dependent [Weinans et al., 1992a; Mullender et al., 1994]. These aspects of validity can be tested directly on the algorithm used.

Mechanistic validity (or physiological validity) implies that the mathematical description of the model, and its variables and parameters, can be related directly to mechanisms and quantities in the real process. For bone-remodeling models the mechanistic validity is inherently poor. For example, only the net amount of bone turnover is captured by the model discussed above, whereas in reality both resorption and formation occur. Although some bone remodeling rules may include more physiological phenomena than others, they are still largely empirical, working with lumped rather than identifyable variables and parameters [Huiskes, 1997]. This is also true for the empirical regulatory model discussed above; its mechanistic validity is not really an issue at the moment, simply because it's not adequately specified yet in its physiological details.

This leaves the predictive validity as the main issue: by what accuracy does the model predict the remodeling patterns occuring in reality? It is evident that the products of the regulatory model above fit reality in a generic sense. It produces trabecular architecture as in real bone, with alignment of trabeculae relative to external loads. When the magnitude of the load is changed, the trabecular thickness adapts, and when its orientation is changed, trabecular orientation adapts accordingly, as implied by Wolff's Law. The characteristic dimensions of the architecture—e.g. trabecular thickness and separation—are largely similar to those in reality. Under particular three-dimensional loading conditions, plates are formed, rather than struts, just as we see in real bone. When loads are reduced, trabeculae reduce in thickness and plates are perforated, as we see in conditions such as in disuse osteoporosis. If trabeculae are disconnected, they disappear, as occurs in reality as well. All these aspects of the model we have investigated in 2-D and 3-D morphologies [Mullender and Huiskes, 1995; Mullender et al., 1996; van Rietbergen et al., 1995]. We have yet to find a general architectural feature in the predictions which is contradicted by reality at large [Huiskes and Mullender, 1997]. However, all these considerations relate to bone in a generic sense; the model is yet to be tested relative to a well-controlled experimental reality. This regulatory model has not shown to be invalid in its predictive

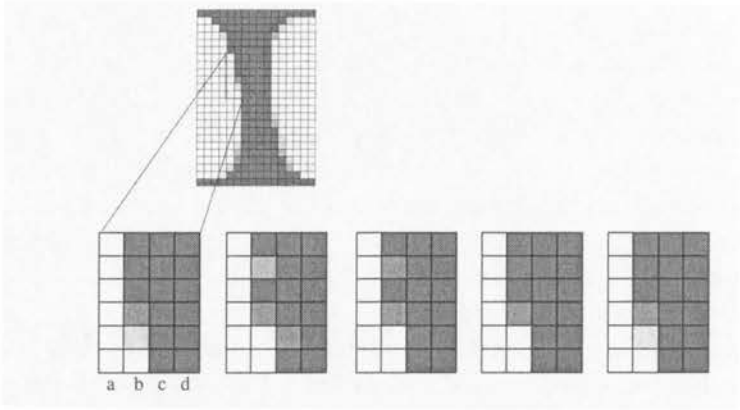


FIGURE 8. The process of bone remodeling, as simulated in the FEA model is clarified in this conceptual scheme. On the left the initial configuration. Then a resorption cavity is created at elements (b,2), simulated by a reduction of m, the relative density of that element, proportional to the fixed amount of bone resorbed per osteoclast. Also at element (b,5) a cavity is created, but because there is not enough bone in that element, element (c,5) is involved as well. In the third and fourth picture it can be seen how the density gradually returns, due to bone formation, until the original situation is restored in the last picture.

capacity for bone-remodeling behavior, but at what point can we actually call it valid?

In general, validation of these kinds of models can be established at several levels:

1. *The qualitative validity of predictions relative to bone-remodeling phenomena at large.* The question addressed here is whether the simulation model produces patterns of bone-mass adaptations which are qualitatively similar to those seen in reality at large. Such a validation effort signifies whether the description implied by the model makes sense at all. If validation at this level is established, the model can be applied for research purposes [Huiskes, 1995a; Huiskes and Mullender, 1997]. An example of this is illustrated in Fig. 8.
2. *The quantitative validity of predictions relative to a population of experimental realities.* Such a validation shows whether the predictions of the simulation model are adequately close to the average or typical results found in the population concerned. The issue to be addressed here is not purely one of numerical precision. If the model would produce the same conclusion about a particular issue as a series of experiments in which this issue is investigated, the model is valid for this purpose, even if the precision is not excellent. If validity at this level can be established, the

simulation model can be applied in concert with experimental ones, for instance to specify later animal or clinical investigations.

3. *The quantitative validity of predictions relative to a single specimen of an experimental population.*
   Validation studies on this level require animal (or patient) specific models and precise evaluations of experimental bone patterns. After the model has shown to produce valid predictions repeatedly at this level, within an acceptable margin of quantitative precision, it can be considered valid, and be used to replace other kinds of experimentation.

To date, virtually all validation efforts for bone remodeling models known- see Huiskes [1997] for an extensive review - were limited to the first level (1), in order to establish whether the models make sense at all. Since a number of years we have been engaged in animal-experimental and clinical validation studies at the second level [2], concerning our simulation models to predict long-term bone remodeling around implants. Recently we also started work on the third level (3). These efforts and their results are summarized in the following pages.

## 5. The introduction of loading frequency

### Remodeling effects of dynamic loading can be analyzed with static finite element analysis

We assume that the osteocytes sense, as a mechanical signal, the typical strain energy density rate (SED-rate) in a recent loading history. We propose that this SED-rate can be determined in a static finite element analysis. In this particular case, we take a uniformly distributed, periodic stress $\sigma_e(t)$ on the external boundary of a bone specimen, cycling between zero and $\sigma$ [MPa], according to

$$\sigma_e(t) = \frac{1}{2}\sigma(1 + \cos\omega t), \tag{5.1}$$

where $\omega = 2\pi f$, with $f$ the frequency [Hz].
The external stress produces stresses and strains within the bone, which, at a given location, are fully characterized by the principal stresses $\sigma_i$ and principal strains $\varepsilon_i$ $(i = 1, 2, 3)$. Assuming linear elastic material behavior, and neglecting inertia effects, these principal stresses and strains are directly proportional to the externally applied stress, and can be written as

$$\sigma_i(t) = \frac{1}{2}c_i\sigma(1 + \cos\omega t) \quad \text{and} \quad \varepsilon_i(t) = \frac{1}{2}e_i\sigma(1 + \cos\omega t), \tag{5.2}$$

where $c_i$ and $e_i$ are principal stress and strain variables independent of time. For the strain energy density (SED) it follows, by definition

$$S(t) = \frac{1}{8}K\sigma^2(1+\cos\omega t)^2, \quad \text{with } K = \sum_{i=1}^{3} c_i e_i. \tag{5.3}$$

The SED-rate is then calculated as

$$R(t) = \frac{dS}{dt} = -\frac{K\sigma^2}{4}(1+\cos\omega t)\,\omega\sin\omega t. \tag{5.4}$$

The osteocytes are assumed to react to the maximal absolute value of the SED-rate. This maximum occurs for $\omega t = \pi/3$, and its value is found from

$$R_m = |R(t)|_{max} = a\sigma^2\omega K, \quad \text{where} \quad a = \frac{3\sqrt{3}}{16} \approx 0.325. \tag{5.5}$$

When the same bone specimen would have been loaded with a constant external stress $\sigma'$, the principal stresses and strains at a given location in the bone would have been

$$\sigma_i(t) = c_i\sigma' \quad \text{and} \quad \varepsilon_i(t) = e_i\sigma'. \tag{5.6}$$

The SED is then calculated as

$$S' = \frac{1}{2}K[\sigma']^2. \tag{5.7}$$

From Eqs. (5.5) and (5.7), it follows that the dynamic SED-rate $R_m$ equals the static $S'$ if (with $\omega = 2\pi f$)

$$\sigma' = \sigma(4a\pi f)^{\frac{1}{2}} \approx 2\sigma f^{\frac{1}{2}}. \tag{5.8}$$

## 6. A unified theory of stress-induced bone modeling and remodeling[5)]

### The Hypothesis

We propose that osteoblast formation is directly enhanced by mechanical stimuli from external loads, but that osteoclast resorption only depends on load in an indirect way (Fig. 9).

We assumed that the mechanical feedback operates through the typical application rate of a recent, cyclic external loading history [Courteix et al.,

[5)] Adapted from Ruimerman, Huiskes, van Lenthe & Janssen, 2001.

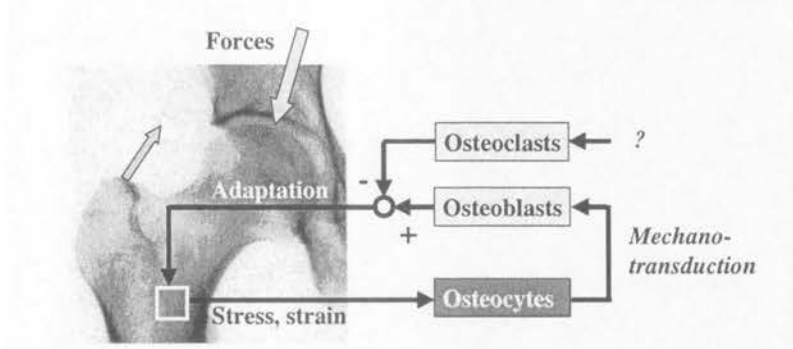


FIGURE 9. The local structure of trabecular bone is mechanically adapted to the orientation and intensity of external forces. The structural optimality is build and maintained by metabolic effector cells, osteoblasts and osteoclasts. Such a regulatory process requires feedback through local mechanosensors and mechanotransduction, the nature of which is unknown, although it is assumed that osteocytes play a role in it.

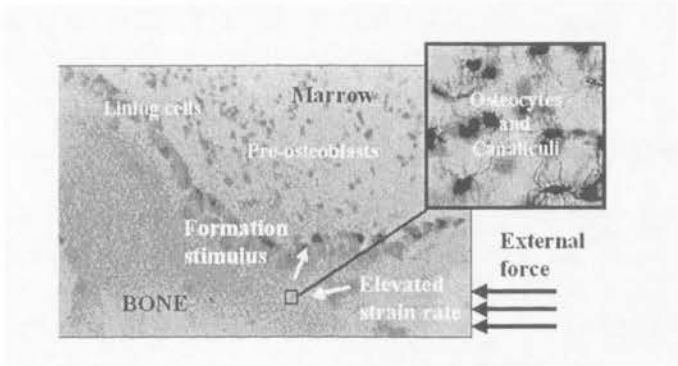


FIGURE 10. It is hypothesized that osteocytes are mechanosensors, sending strain-related signals to lining cells at the bone surface, through the canalicular syncytium. These stimuli are thought to recruit osteoblasts, adding bone to the surface when strains increase (Reproduced from Huiskes et al. [1], Nature 405, with permission).

1998; Mosley & Lanyon, 1998; Liskova & Hert, 1971; Turner et al., 1995; Rubin & Lanyon, 1987], taking account of both amplitude and frequency of the external load. The mechanical load is transferred through the mineralized matrix, where the strain-energy density rate (SED-rate) is appraised by the osteocytes [Carter et al., 1987; Mullender & Huiskes, 1995]. Based on the magnitude of this signal, biochemical stimuli are send to the trabecular surface, through the osteocytic network [Burger & Klein Nulend, 1999; Lanyon, 1993; Skerry et al., 1989; Klein Nulend et al., 1995; Cowin et al., 1991; Knothe Tate et al., 2000] . If the local surface stimulus increases over a

certain threshold value, osteoblasts are recruited, and produce bone matrix until the stimulus decreases below the threshold value (Fig. 10).

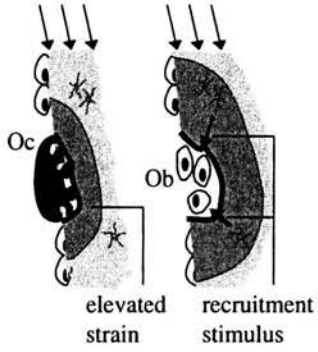


FIGURE 11. The trabecular surface is covered by lining cells, and inside the mineralized tissue are the osteocytes. When an osteoclast (Oc) is recruited to resorb bone, a cavity is made, weakening the trabecula and causing a local elevation of strain. As an effect, it is assumed, osteoblasts (Ob) are recruited by osteocytes, to form bone. During the bone formation process some of the osteoblasts are entrapped in the bone matrix, where they differentiate to new osteocytes. After repair, the remaining osteoblasts become lining cells, covering the new bone surface (adapted from [1]).

In addition to perturbations in external loads, however, osteoclast resorption cavities are likely to provoke local stress concentrations, which may trigger the cascade of mechanical feedback for osteoblastic repair (Fig. 11).

Hence, in the case of homeostatic turnover, without net changes in bone mass ('remodeling'), the osteoblasts just fill the cavities made by the osteoclasts, for which process local stress concentrations (SED-rates) are the cell-coupling factors. In periods of disuse, the osteocytes will not be stimulated, because of the load reduction, and the cavities will not be filled, which leads to bone loss at large. In periods of overloading, bone formation is enhanced, leading to a net gain in bone mass and adaptation.

The motivation for osteoclasts to resorb bone is not really known either, but several hypotheses have been suggested. It is likely that osteoclasts are recruited by signals from the lining cells, which cover the bone surface (Fig. 10) and connect to the osteocytic syncytium [Burger & Klein Nulend, 1999; Chambers & Fuller, 1985; Udagawa et al., 1999]. The cause for these signals to be sent could be related to osteocyte death [Noble et al., 1997] or damage to the osteocytic canaliculi [24,26], as may occur due to microcracks [Burr et al., 1997]. Another hypothesis is that osteoclasts are recruited and activated by bone in disuse [Burger & Klein Nulend, 1999]. For the first hypothesis one would assume that resorption dominates where stresses are

relatively high, and for the second that it dominates where they are relatively low. However, it may be that osteoclast resorption occurs spatially random [Huiskes et al., 2000; Pazzaglia et al., 1997], meaning that it can occur anywhere at the trabecular surface, at any given time. For the specification of the model as outlined here, this was the paradigm we applied, although others were tested as well [Huiskes et al., 2000].

## The governing equation

Figure 12 presents a scheme of the assumed regulatory process to be described mathematically.

Both perturbations in external mechanical loads and osteoclastic cavity formation effect in local perturbations of the SED rates, which sets off a cascade of biochemical reactions, leading to osteoblast recruitment and bone formation. The problem is formulated as a balance of bone mass $M$ in a cancellous bone volume considered. Bone formation and resorption occur at

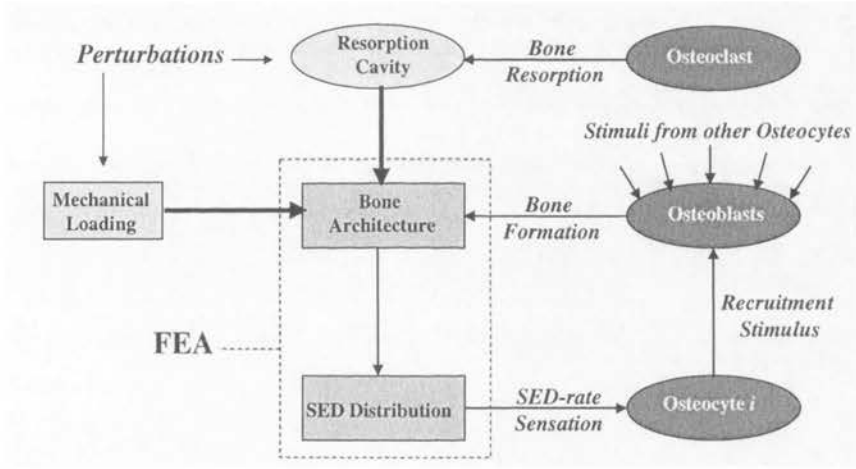


FIGURE 12. A scheme of the proposed regulatory process. Osteoclasts are assumed to resorb bone in a spatially random manner. The cavities they produce alter the local strain-energy density (SED) rate distributions, transferred by the external mechanical loads. These effects can be calculated with finite element analysis (FEA). The SED-rate elevations are sensed by osteocytes, it is assumed, which dissipate a biochemical stimulus for osteoblast bone formation. Apart from the mechanical effects of the resorption cavities, also elevation in external-loading intensity can perturbate the system in producing additional bone. If load is decreased, due to disuse, osteoblastic formation will not be stimulated, and bone mass will reduce through continuous resorption, until a new balance between mass and trabecular strain is reached (Reproduced from Huiskes et al. [1], Nature 405, with permission).

the trabecular surface only. The relationship between $M$ and local remodeling activity is expressed as

$$\frac{dM}{dt} = \frac{dM_{ob}}{dt} + \frac{dM_{oc}}{dt} = \int_{\Omega} \rho_{max} \frac{dm_{ob}}{dt} \delta ds + \int_{\Omega} \rho_{max} \frac{dm_{oc}}{dt} \delta ds = \int_{\Omega} \rho_{max} \frac{dm}{dt} \delta ds, \tag{6.1}$$

where $M$ [g] is the total mass of a cancellous bone volume and $m(x,t)$ is the relative density (between 0 and 1) of a small volume of thickness $\delta$ [mm] under a surface patch $ds$ [mm$^2$] of the trabecular surface $\Omega$. Indices 'ob' stand for osteoblastic activity and 'oc' for osteoclastic activity. The maximal tissue density is a constant $\rho_{max}$ [g/mm$^3$]. The osteoclast and osteoblast terms are evaluated separately, as shown below.

The regulatory process, as depicted in Fig. 12, involves two time frames. First that of a dynamic external load, which varies on the order of seconds, and second the remodeling time, on the order of days. These two frames are separated here [Huiskes, 2000]; remodeling time is denoted by $t$ [$d$ = days], and load-application time by $t^*$ [s]. The spatial coordinate location vector in the bone volume concerned is denoted by $\underline{x}$.

### Spatially random osteoclast resorption

The total amount of bone resorbed per unit of time $R_{oc}$ [g/d], in the bone volume considered, is assumed to be constant, hence

$$\frac{dM_{oc}}{dt} = \int_{\Omega} \rho_{max} \frac{dm_{oc}}{dt} \delta ds = -R_{oc}. \tag{6.2}$$

This can be formulated in the relative density as

$$\frac{dm_{oc}}{dt} = -r_{oc}, \tag{6.3}$$

where $r_{oc}$ [d$^{-1}$] is the change in the relative density of a trabecular surface patch. Where the affected surface patches are located in the total volume considered is determined by chance. The chance that a particular surface patch $ds$ [mm$^2$] becomes subject to osteoclastic cavity formation is denoted by $p_{oc}$ [%].

### Mechanically governed osteoblast recruitment and bone formation

Osteoblast recruitment at a surface patch is assumed to depend on the supply of a chemical messenger, called the formation stimulus, the value of

which is denoted by $P(\underline{x}, t)$ [mol/mm$^2$d]. If the stimulus value is higher than a certain threshold $k_{\text{tr}}$ [mol/mm$^2$d], then this will result in bone formation at the trabecular surface patch proportional to

$$\frac{dm_{\text{ob}}}{dt} = \tau\{P(\underline{x}, t) - k_{\text{tr}}\}, \quad \text{for} \quad P(\underline{x}, t) > k_{\text{tr}}, \tag{6.4}$$

where $\tau$ [mm$^2$/mol·d] is a proportionality factor. If the total stimulus is less than this threshold amount, there will be no bone formation, so

$$\frac{dM_{\text{ob}}}{dt} = 0, \quad \text{for} \quad P(\underline{x}, t) \leq k_{\text{tr}}. \tag{6.5}$$

The value of $P(\underline{x}, t)$ is assumed to be maintained by the osteocytic network, based on the loading of the mineralized tissue and the osteocytes.

### Calculation of the relevant loading characteristics per osteocyte

Osteocytes are assumed to be sensitive to the typical rate of the strain-energy density (SED) in a recent loading history. The SED $S(\underline{x}, t^*)$ [J/mm$^3$] in the location of osteocyte $i$ is denoted by $S_i(t^*)$, and calculated from

$$S_i = \frac{1}{2}\sigma_i : \varepsilon_i, \tag{6.6}$$

where $\sigma_i(t^*)$ is the stress and $\varepsilon_i(t^*)$ the strain tensor, at the location of osteocyte $i$. The calculation of stresses and strains requires the value of Young's modulus of the bone tissue $E_{\text{t}}(\underline{x}, t)$ [MPa], which can be determined from the relative density $m(\underline{x}, t)$ by [Currey, 1988]:

$$E(x, t) = E_{\text{t max}} m(\underline{x}, t)^3, \tag{6.7}$$

where $E_{\text{t max}}$ [MPa] is the tissue Young's modulus at maximal mineralization ($m = 1.0$). The SED-rate $R_i(t^*)$ [J/mm$^3$s] in the location of osteocyte i is calculated as the derivative of the SED in the loading time frame. Using a loading-time averaging procedure over a recent history, specified later, the typical SED rate $R_{ti}(t)$ per osteocyte is determined. Note that this measure is no longer variable in the loading time frame $t^*$, but only in the remodeling time frame $t$; hence its dimension is denoted as [J/mm$^3$].

### Osteocyte signaling as an effect of loading rate

Based on the loading-rate signal, the osteocyte $i$ is assumed to produce a biochemical messenger, a bone formation stimulus of value $p_i(t)$ [mol/d], subject to its mechanosensitivity $\mu_i$ [mol·mm$^3$/J.d], as

$$p_i(t) = \mu_i R_{ti}(t). \tag{6.8}$$

This stimulus is sent through the canaliculi, towards the trabecular surfaces. In this process it is assumed to reduce in strength with increasing distance $d_i$ [$\mu$m] between osteocyte $i$ and location $\underline{x}$, according to [Mullender & Huiskes]

$$f_i(\underline{x}) = e^{-d_i(\underline{x})/D}. \tag{6.9}$$

In this function $D$ [$\mu$m] is the decay constant, the distance from the osteocyte $d_i$ at which $f_i$ reduced from 1.0 to 0.37 (Fig. 13).

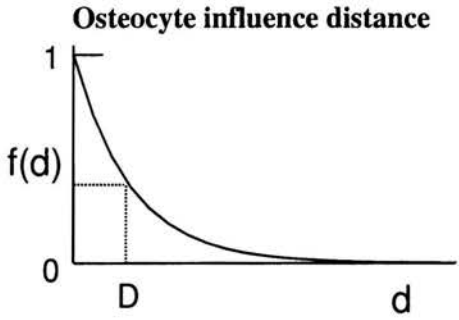


FIGURE 13. The remodeling stimulus, sent to the bone surface by an osteocyte, as an effect of its loading signal, is assumed to decay exponentially over distance. At a distance D (mm) away the stimulus is reduced in intensity to 37%. It turns out that the parameter D controls average trabecular thickness, for a given external force [7].

Only osteocytes less than $d_{\text{infl}}$ [$\mu$m] removed from a surface patch were assumed to have influence on its stimulus value. The total bone formation stimulus value $P(\underline{x}, t)$ at the trabecular surface (Eq. 6.4), maintained by stimuli from all osteocytes, can now be written as

$$P(\underline{x}, t) = \sum_{i=1}^{n} f_i(\underline{x}) p_i(t), \tag{6.10}$$

where $f_i(x)$ is the influence function and $p_i(t)$ the stimulus from osteocyte $i$, summed over the $n$ osteocytes less than $d_{\text{infl}}$ removed from $\underline{x}$.

### Combined bone formation and bone resorption

The mass balance (Eq. 6.1) of bone formation and resorption can now be summarized as

$$\begin{aligned} \frac{dm}{dt} &= \tau\{P(\underline{x}, t) - k_{\text{tr}}\} - r_{\text{oc}} \quad \text{for} \quad P(\underline{x}, t) > k_{\text{tr}}, \\ \frac{dm}{dt} &= -r_{\text{oc}} \quad \text{for} \quad P(\underline{x}, t) < k_{\text{tr}}, \end{aligned} \tag{6.11}$$

where, with Eqs. (6.8) and (6.10),

$$P(\underline{x},t) = \sum_{i=1}^{n} f_i(\underline{x})\mu_i R_{ti}(t). \tag{6.12}$$

### Computer-simulation model

The mathematical equations were transformed to numerical algorithms in combination with the finite element analysis (FEA) code MARC (Marc Analysis Corporation, Palo Alto, CA, USA). Due to the size of the problem, simulations had to be limited to a 2-dimensional model of a small bone volume, loaded at the edges by a tensile and compressive principal stress profile of the form

$$\sigma(\underline{t}) = \sigma(1 + \cos 2\pi f\underline{t}), \tag{6.13}$$

where $\sigma$[MPa] is the amplitude and $f$ [Hz] the frequency in the loading time frame $\underline{t} = t^*$ [s]. For the typical SED loading rate $R_{ti}$ (Eqs. (6.8) we selected the maximal one in this dynamic signal. In this case the problem can be solved as a static FEA in the remodeling time frame, with an external stress $\sigma'$. The static SED $S_i$ calculated in this way is equal to the maximal SED-rate caused by the dynamic signal, subject to $\sigma' = 2\sigma f^{1/2}$.

The computer simulation was conducted as an iterative process in computer time, in which the relative density m per element was regulated between 0.01 and 1.0 (Eq. (6.11). An independent network of osteocyte locations was defined. Per iteration the FEA code evaluated the stress and strain components in the integration points of each element. By interpolation, the stresses, strains and SED's (hence also the maximal SED rates) in the locations of the osteocytes were determined. The stimulus signals and the changes in the density of the elements at the trabecular surface were determined depending on a calculated time step. In every time step, the elements located at the trabecular surface can undergo a change in relative density $\Delta m$ dependent on the local value of $P(\underline{x},t)$, according to Eq. (6.4). To ensure stability the time step $\Delta t$ was calculated which renders the maximal density change during one increment less than $(\Delta m)_{\max}$, from

$$\Delta t = \frac{(\Delta m)_{\max}}{\tau P_{\max}}, \tag{6.14}$$

where $P_{\max}$ is the maximal stimulus value occurring anywhere in the mesh and $\tau$ is the proportionality factor (Eq. (6.4).

In every iterative time step $p_{oc}$ [%] of the surface elements were reduced in relative density to simulate osteoclastic resorption by a fixed amount of

$\triangle v$ [mm$^3$] per site. The locations of these elements were selected stochastically by a Monte Carlo number generator. Elements or element groups unconnected to the trabecular structure at large were detected and removed. Figure 8 gives a graphic representation of the procedure. Since only a limited volume of bone could be analyzed, boundary conditions are important, where it concerns both elastic deformations and signal distribution. Surfaces close to the edge of the mesh, and particularly those in the corners, have a reduced osteocytic environment to receive stimuli from, as compared to those in the center of the mesh. A correction of the stimulus is made by a factor $K$ in these regions. In order to impose even deflection at the edges of the model, plates were added of maximal relative density, which did not remodel (Fig. 14).

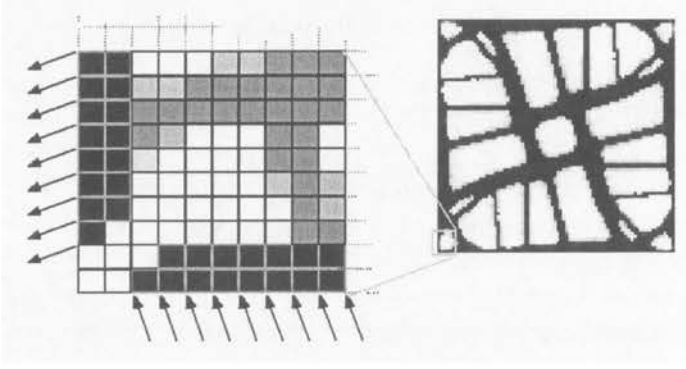

FIGURE 14. In the detailed, enlarged view of the FEA model on the left the stiff side plates are seen, which don't partake in the remodeling process. They are required to ensure proper boundary conditions for the load to be transferred evenly and to keep the boundaries straight.

## Application

The model was applied to a square domain of 2×2 mm and thickness 0,02 mm. This domain was described by 80×80 rectangular four-node elements [Mullender & Huiskes]. The thickness of the side plates (Fig. 12) was 2 elements, equal to 0.050 mm. The osteocyte density was about 1600/mm$^2$ bone [Mullender et al., 1996] (one in the center of each bone-filled element) and the influence parameter $D$ equaled 100 $\mu$m [Mullender & Huiskes]. The maximal Young's modulus of the trabecular tissue was taken as $E_{\mathrm{t\,max}} = 5.000$ [MPa] [van Rietbergen et al., 1999].

The probability of osteoclastic activation per surface patch was chosen arbitrarily at $p_{\mathrm{oc}} = 10\%$ per iteration, which equals approximately 400 times

per time unit per square millimeter. The constant amount of bone volume that is resorbed by one osteoclast was $\triangle v = 6.25 \cdot 10^{-6}$ mm$^3$ [Kanis, 1997]. The threshold value $k_{\mathrm{tr}} = 0.3$ mol/mm$^2$d and the sensitivity of the osteocytes was set to $\mu_i = 1.0$ mol$\cdot$mm$^3$/J$\cdot$d. The proportionality factor $\tau = 1\,\mathrm{mm}^2/\mathrm{mol}\cdot\mathrm{d}$. An external principal-stress loading configuration with stress-amplitudes $\sigma_1 = 2$ MPa and $\sigma_2 = -2$ MPa [Huiskes et al., 1992], and a frequency of 1 Hz, was imposed; hence, the substitute static stress was 4 MPa, in tension and compression). The orientation of the principal stresses was 30 degrees counterclockwise, relative to perpendicular. Five series of computations were performed. Two of those were iterations from alternative initial architectures, conducted until an architectural equilibrium was reached (homeostasis), simulating growth and remodeling. The third were iterations relative to the homeostatic architecture, after rotation of the external load, simulating adult adaptation. In the fourth the external loads were reduced by 20%, relative to the homeostatic configuration, simulating disuse, and in the fifth they were increased by 20%, simulating overloading.

## Results

From two different initial configurations the architectures converged to similar forms, characterized by a particular trabecular thickness, and the trabecular orientation aligned with the external loads (Fig. 15).

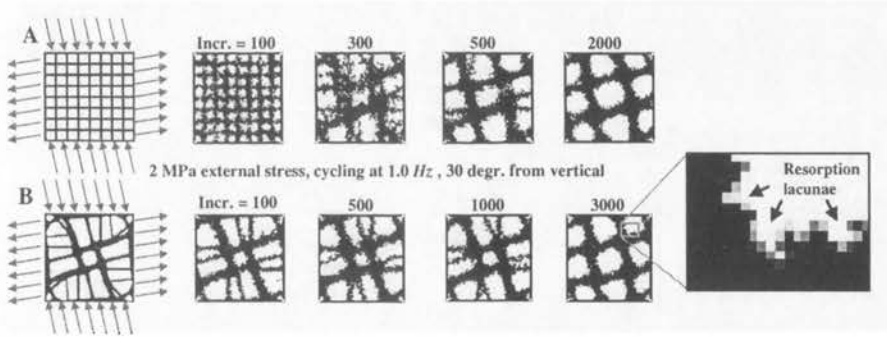


FIGURE 15. Development of bone architecture in the simulation model, started from two different initial configurations, A and B, shown in a few iterations. Eventually, homeostatis is obtained, where only 'remodeling' occurs, during which the architecture at large does not change anymore, although resorption cavities are still made and filled, as illustrated by the blown-up picture (adapted from [1]).

The first initial configuration (A) was an arbitrary grid, similar to what was used by Mullender and Huiskes [1995]. The second (B) was a converged architecture obtained by the same authors. The simulations were continued

until the architecture remained largely intact between iterations, although there is no stage of 'equilibrium', as the process of remodeling, in which resorption cavities are created by 'osteoclasts' and repaired again by osteoblasts, continues (Fig. 15). Hence, there is no precisely defined end to the process. The simulations required about 6 hours computing per 1,000 iterations on a workstation. Note that the time steps are variable, as explained above, so there is no direct relationship between number of iterations and (computer) time. Configuration A needed more growth and adaptation than configuration B, as can be seen in the development of the bone volume fractions (Fig. 16a), showing an overshoot for A.

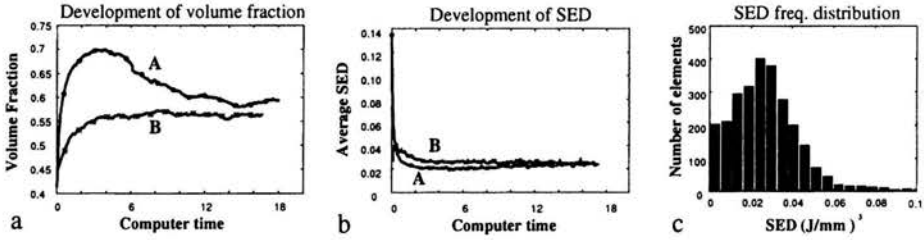


FIGURE 16. Development over time of volume fraction (a) and average SED (b) during the simulations A and B of Fig. 15. Initial configuration A is less efficient than B, and needs more extensive adaptation. In both cases, however, the average SED reaches the final value relatively fast. In the homeostatic architectures, which are virtually identical, the SED is not homogeneously distibuted (c), but shows a pattern similar to what was found using mFEA analyses of a proximal dog femur [45].

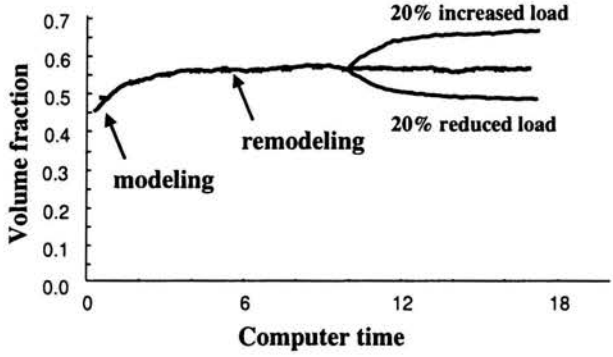


FIGURE 17. The time development of volume fraction in simulation B of Fig. 15, augmented by the developments for 20% increased and reduced loading amplitudes.

The average SED in the mesh converged to its 'final' value relatively rapid in both cases (Fig. 16b). We estimate that one unit of computer time is approximately equivalent with one year of real time. In the homeostatic configuration, when only remodeling occurs, the strain-energy density (SED) varies between 0 and about 0.06 J/mm$^3$, although a few elements have higher values (Fig. 16c). The average SED value is around 0.03 [J/mm$^3$], if only non-surface elements are considered.

To simulate adaptation to alternative external loads, we changed both the amplitude and the orientation of loads applied to the 'final' architecture of simulation B. Enlarging the amplitude by 20% gradually thickened the trabeculae, to an eventual increase in volume fraction of 17.5% (Fig. 17).

Reducing it by 20% led to thinning of trabeculae, to a decreased volume fraction by 15.8% (Fig. 17). Rotating the external loads from 30 degrees angles to the horizontal and the vertical to a perpendicular orientation, gradually re-aligned the trabeculae accordingly (Fig. 18).

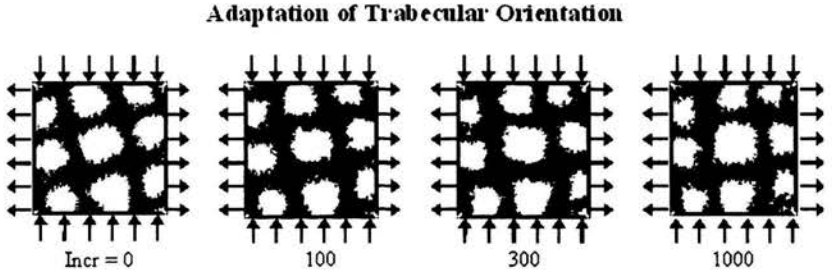


FIGURE 18. When the orientation of the external loads is changed relative to the homeostatic architecture (Fig. 15), trabecular orientation is adapted accordingly.

## Discussion

The regulatory model we developed into a computer-simulation procedure relates input (bone-loading rate) to output (growth, maintenance and adaptation of trabecular architecture by the bone cells), taking a giant step over the complex biochemical processes of bone metabolism. The cell-signaling mediators in metabolism, and certainly their influence on mechanical adaptation, are largely unknown, despite new information obtained in the recent past [Burger & Klein Nulend, 1999]. But even if we knew all the actors, their relationships to the bone modeling and remodeling processes still evade us, particularly in a quantitative sense. In our model, these relationships were postulated in their simplest form. Hence, the model is a crude one, but it

does relate external bone loading to maintenance and adaptation of trabecular morphology in a quantitative way, taking account of the known effector cell functions – the osteoclasts and osteoblasts, while capturing the assumed mechanosensory role for the osteocytes in a quantitative way as well. The mechanosensory and transductory pathways captured in the model are hypothetical, but not really controversial, as witnessed by a recent review from Burger and Klein-Nulend [1999]. Although in fact nothing is known about the validity of the quantitative relationships we postulated for the signaling functions along this pathway, we have at least some confidence that the assumed paradigm that couples local bone formation to external loading makes sense.

Much more uncertain is the formulation we used to describe osteoclastic resorption. There is an old intuitive paradigm suggesting that osteoclasts resorb disused bone, and osteoblasts augment overloaded bone, thus making them 'comrades at arms' in bone adaptation; our earlier model [Mullender & Huiskes, 1995], considering net bone-mass regulation only (hence, 'modeling' [Frost, 1987]) was based on it. However, this does not capture or explain remodeling. Why would bone be replaced in the osteoclast lacunae if the area is disused? Another argument against it is that bone resorption is evolutionary advantageous when it removes damaged bone; i.e. bone with microcracks [Burr et al., 1997, Mori et al., 1997]. Microcracks are more likely to occur where bone is overloaded than where it is disused. Results reported from vertebral rat studies by Pazzaglia et al. [1997] actually showed that resorption rates did not change in disuse. Although in recent years much information has been obtained about the cell-signaling pathways through which osteoclasts are attracted from the marrow and activated, what triggers the onset of these processes is not known [Chambers, 1998; Burger & Klein Nulend, 1999; Chambers & Fuller, 1985; Udagawa et al., 1999]. Mediators for osteoclastic activation are probably produced by cells from the osteoblastic lineage; i.e. osteoblasts, osteocytes and/or lining cells [Udagawa et al., 1999]. It can be hypothesized that such signals are generated by osteocytes or lining cells in case of micro-damage in the bone matrix, or damage to the osteocytes themselves [Skerry et al., 1989; Noble et al., 1997; Verborgt et al., 2000; Vashishth et al., 2000]. Alternatively, it may be that these signals are initialized by lining-cells when their communication with the osteocytic network is interrupted by mechanical damage or lack of mechanical 'pumping' [Burger & Klein Nulend, 1999]. What mattered for our model and its purpose was not so much to know if and how the osteoclasts would be attracted, but rather where they become active. We assumed that micro damage in the bone matrix triggers osteoclast activation, and that the occurrence of damage is spatially random, i.e. that it can occur anywhere at

any time, while the amount of damage generated in a given volume during a finite time span is constant. This assumption is not unreasonable, since strain peaks in the various trabeculae in an area do not vary excessively, seen over a typical daily usage [van Rietbergen et al., 1999], while tissue strength is probably quite variable, due to the composite nature of the submicroscopic lamellar structure [Choi & Goldstein, 1992]. Anyway, because indications for disuse-driven osteoclastic resorption in the literature cannot be ignored, we repeated the simulations based on the assumption that the local probability for resorption would be SED dependent, with a higher chance for disused areas [Huiskes et al., 2000]. We found similar effects, be it that the modeling simulation processes were accelerated. This is not surprising, because in this case the osteoclasts 'assist' the osteoblasts in shaping form in accordance with mechanical demands, while they do not in the case of spatially random resorption.

It is virtually certain that not the static, but rather the dynamic aspects of bone loading produce metabolic responses. We were able to capture this in the model, making use of the vastly different time frames of dynamic loading and bone metabolism, which enables the inclusion of loading amplitude and frequency in static FEA. But this 'trick' works only for sinusoidal external loads of the same frequencies; maybe Fourier analysis may help to generalize that to more involved loading patterns in the future. The model was two-dimensional, and small relative to trabecular-bone volume in real bone. Hence, the conditions necessary to consider this volume as a continuum, i.e. to have at least 5 trabeculae across its dimensions [Harrigan et al., 1988], were not necessarily fulfilled. By applying smart boundary conditions for both deformations and signal transduction we could obtain realistic conditions for the individual trabeculae. Finally, many parameter values had to be guessed at. Hence, the model was crude and simple also in its computational qualities. Development towards three-dimensional whole bones is possible in principle, but restricted by contemporary computer capacity.

The most significant result of this work is in the combination of model simplicity and its incredible stability. We know that trabecular architecture is modulated by external forces, and we also know that its morphology is very consistent in all vertebrates. Our model proves that it can be build, maintained and adapted simply by spatially random resorption and strain-related formation, by cells that have no other communication than governed through mechanics. Our model also proves that the morphologically different cell expressions of growth, maintenance and mechanical adaptation do not necessarily imply differences in cell function; they can all be captured by the same regulatory principles. This also means that there is not necessarily a difference in 'modeling' and 'remodeling' from a cell regulatory point of view.

This can also be inferred from results of morphometric studies in rats [Chow et al., 1993], which showed that osteoclastic resorption and osteoblastic formation occur together also during growth. Recent work of Parfitt et al. [2000] points in that direction as well. We believe that the bone cells do not have to know what stage the organism is at. All they have to do is react normally to environmental stimuli. Or, in other words, genetics make them work, but stimuli determine to what it leads.

Quite a few modeling and remodeling algorithms were presented in the literature in recent years. Some of those were briefly mentioned here, as far as they were relevant for the development of the present model. We think this is not the place for an extensive review of the others. For the interested reader, however, we refer to the survey article of Hart and Fritton [1997].

The fact that our proposed regulatory algorithm produces bone-like architectures from loading does not imply that the hypotheses on which it is based are true. It only proves that they could be true. In this sense, the model falls within the tradition of attempts to explain forms in nature from simple regulatory processes, driven by environmentally related stimuli, as reviewed by Stewart [1998]. Invariably, the mathematical descriptions of these processes are basically simple, and stable, despite their multiple degrees of freedom and nonlinear relationships. Much of the variability in biology is due simply to the nature of nonlinear dynamics, and thus can be simulated. One could say that our results provide a challenge, rather than an answer. It is normal in physics research of natural phenomena that quantitative theories, based on earlier experimentation and observations, drive future experimentation; the theory provides a direction for experimentation. Hence, in this sense our results present a challenge and a direction for experiments. Computer simulation was proposed as the "Third Method of Science", after theoretical and empirical research [Kelly, 1998]. It is now increasingly used as a research tool to test new theories and paradigms, in biochemistry and biophysics. If a regulatory paradigm works in computer simulation, it might work in reality as well; if it does not, it is likely to be the wrong paradigm.

To actually validate the theory in a quantitative sense, and to apply it for valid predictions that are useful and falsifiable, its application in a 3-dimensional geometry is required. Computer capacity is a limiting factor for this requirement and it is currently not possible to simulate bone modeling and remodeling in complete bones at the trabecular level. In order to test whether our theory can produce trabecular-like structures in three dimensions, with morphological characteristics in a quantitative realistic range, for actual trabecular bone, we developed a 3-dimensional computer simulation model that can be applied to a small domain of bone tissue. Preliminary results show that the theory mimics the realistic morphological expressions

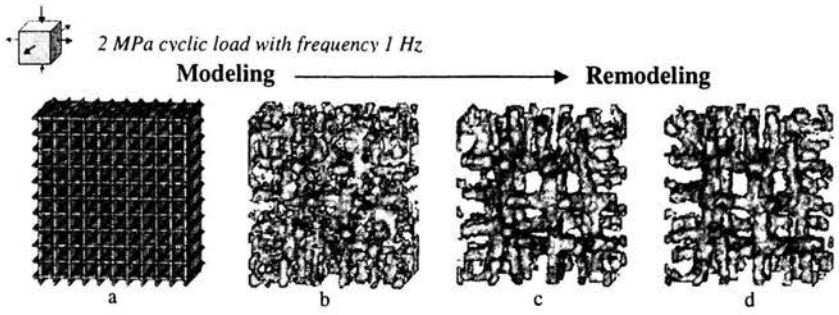


FIGURE 19. Development of a 3-dimensional trabecular architecture as governed by external forces, starting from the porous initial configuration illustrated in (a), and the configuration after 10, 30 and 200 iterations (b-d).

of bone cell metabolism in a robust way, in growth, adaptation and remodeling, when applied to a small cube ($2 \times 2 \times 2\,\mathrm{mm}^3$) of bone tissue with external loads imposed. When started from an initial porous configuration, the model produced structures with trabecular alignment in the loading direction (Fig. 19), while volume fraction correlated to the magnitude of the external loads.

The model described the growth as well as adaptation of complex 3-dimensional structures that are similar to actual trabecular bone. The architectures produced are remarkably stable, while the remodeling process proceeds.

Initially, theories for bone adaptation related bone density changes directly to mechanical, strain derived variables as effects of external forces. The computational simulation models based on these theories proved useful tools for prosthetic design. They were empirical models on a macroscopic level and the underlying biological processes involved were not taken into account. In the past decade the focus has shifted from biomechanics to mechanobiology, as it is likely that actual intervention in metabolic processes, to cure bone diseases, will be based on understanding the relationship between mechanics and cell biology. Understanding of bone biology has improved enormously in the past 15 years. This combined with increased computer capacities and efficient finite element algorithms has enabled the application of realistic theories, including the main aspects of bone biology. The theory relates cellular activity in bone modeling and remodeling to external forces and explains adaptive behavior of trabecular bone at a microscopic level. Although the most important relationships are captured in the theory, it should still be considered as a framework. The relationships are captured in simple mathematical equations, but actually encompass complex biological processes, the biochemical

components of which are largely unknown. Nevertheless, the computational models based on the theory will enable us to investigate the morphological consequences of alternative loading conditions, metabolic disorders and their pharmaceutical interventions. They are useful tools for the development and investigation of hypotheses and for efficient design of experiments. Potentially they are useful for prosthetic design, as the adaptation of bone tissue to alternative mechanical environments can be pre-clinically tested. They can also be used in the development of treatment methods of osteoporosis, either based on physical exercise or in combination with pharmaceutics. In the near future the 3D computational model will be used in order to investigate questions like: can the morphological changes seen in senile osteoporosis be explained by reduced physical activity alone? Can anti-resorptive drug administration prevent loss of bone tissue and preserve trabecular connectivity, and at what stage should such a treatment start? Another area where the model can be applied is in postmenopausal osteoporosis. Can the theory mimic the phenomena observed in postmenopausal osteoporotic bone (loss of bone density and trabecular connectivity at a higher remodeling rate) and what is the role of mechanical coupling between osteoclasts and osteoblasts for this condition? Can osteoporosis be an effect of reduced osteocyte mechanosensitivity? Can the morphology of osteopetrotic bone be predicted as an effect of dis-functioning osteoclasts? Can the loss of trabeculae in older ages be prevented? Could the effects of physical activity be replaced by high frequency vibrations? Can trabecular and cortical (osteonal) bone modeling and remodeling processes be described with the same theory, and can the theory explain the transformation of trabecular into cortical bone from mechanobiological stimuli, as it occurs in growth? These are all important questions in bone biology and pharmacology.

## References

1. T. ADACHI, K. TSUBOTA, Y. TOMITA, S.J. HOLLISTER, Trabecular surface remodeling simulation for cancellous bone using microstructural voxel finite element models, *J. Biomech. Engr.*, Vol. 123, 403-409, 2001.

2. D.A. BAILEY, H.A. MCKAY, R.L. MIRWALD, P.R.E. CROCKER, R.A. FAULKNER, A six-year longitudinal study of the relationship of physical activity to bone mineral accrual in growing children: the university of saskatchewan bone mineral accrual study, *J. Bone Miner.*, Vol.14, pp.1672-1679, 1999.

3. G.S. BEAUPRÉ, T.E. ORR, D.R. CARTER, An approach for time-dependent bone modeling and remodeling – theoretical development, *J. Orthop.*, Vol.8, pp.651-661, 1990.

4. A.L. BRONCKERS, W. GOEI, G. LUO, G. KARSENTY, R.N. D'SOUZA , D.M. LYARUU, E.H. BURGER, DNA fragmentation during bone formation in neonatal

rodents assessed by transferase-mediated end labeling, *J. Bone Miner.*, Vol.11, pp.1281-1291, 1996.

5. J.A. BUCKWALTER, D. MOWER, R. UNGAR, J. SCHAEFFER, B. GINSBERG, Morphometric analysis of chondrocyte hypertrophy, *J. Bone Surg [Am]*, Vol.68, pp.243-255, 1986.

6. E.H. BURGER, J. KLEIN-NULEND, J.P. VELDHUIJZEN, Mechanical stress and osteogenesis in vitro, *J. Bone Miner.*, Vol.7, pp.397-401, 1992.

7. E. H. BURGER, J. KLEIN-NULEND, Mechanotransduction in bone – role of the lacuno-canalicular network, *FASEB J.*, Vol.13, pp.101-112, 1999.

8. E. H. BURGER, J. KLEIN-NULEND, Microgravity and bone cell mechanosensitivity, *Bone (Suppl.)*, Vol.22, pp.127-130, 1998.

9. D. B. BURR, M. FORWOOD, D. P. FYHRIE, R. B. MARTIN, C. H. TURNER, Bone microdamage and skeletal fragility in osteoporosis and stress fractures, *J. Bone Miner.*, Vol.12, pp.6-15, 1997.

10. D.R. CARTER, Mechanical loading histories and cortical bone remodeling, *Calcif. Tissue Int.*, Vol.36, pp.19-24, 1984.

11. D.R. CARTER, Mechanical loading history and skeletal biology, *J. Biomech.*, Vol.20, pp.1095-1109, 1987.

12. D.R. CARTER, W.C.HAYES, The behavior of bone as a two-phase porous structure, *J. Bone Jt. Surg.*, Vol.59-A, pp.954-962, 1977.

13. D.R. CARTER, D. P. FYHRIE, R. T WHALEN, Trabecular bone density and loading history: Regulation of connective tissue biology by mechanical energy, *J. Biomechanics*, Vol.20, pp.785-794, 1987.

14. D.R. CARTER, D.P. FYHRIE, T.E. ORR, Relationships between loading history and femoral cancellous bone architecture, *J. Biomechanics*, Vol.22, pp.231-244, 1989.

15. T.J. CHAMBERS, The direct and indirect effects of estrogen on bone formation, *Adv. in Organ. Biol.*, Vol.5B, pp.627-638, 1998.

16. T.J. CHAMBERS, K. FULLER, Bone cells predispose bone surfaces to resorption by exposure of mineral to osteoclastic contact, *J. Cell Sci.*, Vol.6, pp.155-165, 1985.

17. K. CHOI, S. A. GOLDSTEIN, A comparison of the fatigue behavior of human trabecular and cortical bone tissue, *J. Biomechanics*, Vol.25, pp.1371-1381, 1992.

18. J. W. M. CHOW, S. BADVE, T. J. CHAMBERS, Bone formation is not coupled to bone resorption in a site-specific manner in adult rats, *Anat. Rec.*, Vol.236, pp.366-372, 1993.

19. T.E. CIARELLI, D.P. FYHRIE, M.B. SCHAFFLER, S.A. GOLDSTEIN, Variations in three-dimensional cancellous bone architecture of the proximal femur in female hip fractures and in controls, *J. Bone Miner. Res.*, Vol.15, pp.32-40, 2000.

20. D. COURTEIX, E. LESPESSAILLES, S. LOISEAU PERES, P. OBERT, P. GERMAIN, C. L. BENHAMOU, Effects of physical training on bone mineral density in prepubertal girls: a comparative study between impact-loading and non-impact-loading sports, *Osteopor. Int.*, Vol.8, pp.152-158, 1998.

21. S.C. COWIN, Bone poroelasticity, *J. Biomech.*, Vol.32, pp.217-238, 1999.

22. S.C. COWIN, D.H. HEGEDUS, Bone remodeling I: Theory of adaptive elasticity, *J. Elasticity*, Vol.6, 313-326, 1976.

23. S.C. COWIN, K. FIROOZBAKHSH, Bone Remodeling of Diaphyseal surfaces under constant load: theoretical predictions, *J. Biomechanics*, Vol.14, pp.471-484, 1981.

24. S.C. COWIN, R.T. HART, J.R. BABER, D.H. KOHN, Functional adaptation in long bones: Establishing in vivo values for surface remodeling rate coefficients, *J. Biomechanics*, Vol.18, pp.665-684, 1985.

25. S.C. COWIN, L. MOSS-SALENTIJN, M.L. MOSS, Candidates for the mechanosensory system in bone, *J. Biomech. Eng.*, Vol.113, pp.191-197, 1991.

26. S.C. COWIN, S.WEINBAUM , Y. ZENG, A case for bone canaliculi as the anatomical site of strain generated potentials, *J. Biomech.*, Vol.28, pp.1281-1297, 1995.

27. J.D. CURREY, The effect of porosity and mineral content on the Young's modulus of elasticity of compact bone, *J. Biomech.*, Vol.21, pp.131-139, 1988.

28. L.A. FELDKAMP, S.A. GOLDSTEIN, A.M. PARFITT, G. JESION, M. KLEEREKOPER, The direct examination of three-dimensional bone architecture in vitro by computed tomography, *J. Bone Miner. Res.*, Vol.4, pp.3-11, 1989.

29. K. FIROOZBAKHSH, S.C. COWIN, An analytical model for Pauwels' functional adaptation mechanism in bone, *J. Biomech. Eng.*, Vol.103, pp.247-252, 1981.

30. H.M. FROST, *Bone Biodynamics*, pp.315-333, Brown and Co., Boston, 1964.

31. H.M. FROST, Vital biomechanics. Proposed general concepts for skeletal adaptations to mechanical usage, *Calcif. Tissue Int.*, Vol.42, pp.145-156, 1987.

32. D.P. FYHRIE, D.R. CARTER,A unifying principle relating stress to trabecular bone morphology, *J. Orthop. Res.*, Vol.4, pp.304-317, 1986a.

33. D.P. FYHRIE, D.R. CARTER, Prediction of cancellous bone apparent density with 3D stress analysis, *Transactions 32nd Annual Orthopaedic Research Society*, pp.331, 1986b.

34. A. HAAIJMAN, R.N. D'SOUZA, A.L.J.J. BRONCKERS, S.W. GOEI, E.H. BURGER, OP-1 (BMP-7) affects mRNA expression of type I, II, X collagen, and matrix Gla protein in ossifying long bones in vitro, *J. Bone Miner. Res.*, Vol.12, pp.1815-1823, 1997.

35. T.P. HARRIGAN, M. JASTY, R.W. MANN, W.H. HARRIS, Limitations of the continuum assumption in cancellous bone, *J. Biomech.*, Vol.21, pp.269-275, 1988.

36. R.T. HART, Bone modeling and remodeling: theories and computation, *Bone Biomechanics Handbook*, Vol.31, pp.1-42, S.C. Cowin, Boca Raton, CRC-Press, 2001.

37. R.T. HART, Introduction to finite element based simulation of functional adaptation of cancellous bone, *Forma*, Vol.12, pp.277-299, 1997.

38. R.T. HART, D.T. DAVY, K.G. HEIPLE, A computational method for stress analysis of adaptive elastic materials with a view toward applications in strain-induced bone remodeling, *J. Biomech. Engr.*, Vol.106, pp.342-350, 1984.

39. R. HUISKES, The law of adaptive bone remodeling: a case for crying Newton?, in: *Bone Structure and Remodeling*, A. Odgaard and H. Weinans, (Eds.), pp.15-24, World Scientific Publishing, Singapore, River Edge, London, 1995a.

40. R. HUISKES, Orthopaedic research in Europe, *European Orthopaedics (EFORT Bulletin)*, Vol.5, November, pp.1-5, 1996a.

41. R. HUISKES, Simulation of self-organization and functional adaptation in bone, in: *Biomechanik des menslichen Bewegungsapparatus*, E. Schneider (Ed.), *Der Unfallchirurg*, Vol.261, November, pp.299-320, 1997.

42. R. HUISKES, If bone is the answer, then what is the question?, *J. Anatomy*, Vol.197, pp.145-156, 2000.

43. R. HUISKES, S.J. HOLLISTER, From structure to process, from organ to cell: recent developments of FE-analysis in orthopaedic biomechanics, *J. Biomech. Engr.*, Vol.115, pp.520-527, 1993.

44. R. HUISKES, M.G. MULLENDER, Adaptive bone remodeling in cyberspace: tricks and treats, *Forma*, Vol.12, pp.305-312, 1997.

45. R. HUISKES, H. WEINANS, H.J.GROOTENBOER, M. DALSTRA, B. FUDALA, T.J. SLOOFF, Adaptive bone-remodeling theory applied to prosthetic-design analysis, *J. Biomech.*, Vol.20, pp.1135-1150, 1987.

46. R. HUISKES, H. WEINANS, B. VAN RIETBERGEN, The relationship between stress shielding and bone resorption around total hip stems and the effects of flexible materials, *Clin. Orthop.*, Vol.274, pp.124-134, 1992.

47. R. HUISKES, R. RUIMERMAN, G.H. VAN LENTHE, J.D. JANSSEN, Effects of mechanical forces on maintenance and adaptation of form in trabecular bone, *Nature*, Vol.405, pp.704-706, 2000.

48. E.B. HUNZIKER, R.K. SCHENK, Physiological mechanisms adopted by chondrocytes in regulating longitudinal bone growth in rats, *J. Physiol.*, Vol.414, pp.55-71, 1989.

49. C.R. JACOBS, J.C. SIMO, G.S. BEAUPRÉ, D.R. CARTER, Adaptive bone remodeling incorporating simultaneous density and anisotropy considerations, *J. Biomech.*, Vol.30, pp.603-613, 1997.

50. C.R. JACOBS, C.E. YELLOWLEY, B.R. DAVIS, Z. ZHOU, J.M. CIMBALA, H.J. DONAHUE, Differential effect of steady versus oscillating flow on bone cells, *J. Biomech.*, Vol.31, pp.969-976, 1998.

51. J.A KANIS, Osteoporosis, *Blackwell Healthcare Communications Ltd*, London, 1997.

52. T.M. KEAVENY, E.F. WACHTEL, C.M. FORD, W.C. HAYES, Differences between the tensile and compressive strengths of bovine tibial trabecular bone depend on modulus, *J. Biomech.*, Vol.27, pp.1137-1146, 1994.

53. J. KELLY, The third culture, *Science*, Vol.279, pp.992-993, 1998.

54. J. KERNER, R. HUISKES, G.H. LENTHE, H. VAN WEINANS, B. RIETBERGEN, C.A. VAN ENGH, A.A. AMIS, Correlation between pre-operative periprosthetic bone density and post-operative bone loss in THA can be explained by strain-adaptive remodelling, *J. Biomech.*, Vol.32, pp.695-703, 1999.

55. T. KIRSCH, H.D. NAH, I.M. SHAPIRO, M. PACIFICI, Regulated production of mineralization-competent matrix vesicles in hypertrophic chondrocytes, *J. Cell. Biol.*, Vol.137, pp.1149-1160, 1997.

56. J. KLEIN-NULEND, J.P. VELDHUIJZEN, E.H. BURGER, Increased calcification of growth plate cartilage as a result of compressive force in vitro, *Arth. Rheum.*, Vol.29, pp.1002-1009, 1986.

57. J. KLEIN-NULEND, A. VAN DER PLAS, C.M. SEMEINS, N.E. AJUBI, J.A. FRANGOS, P.J. NIJWEIDE, E.H. BURGER, Sensitivity of osteocytes to biomechanical stress in vitro, *FASEB J.*, Vol.9, pp.441-445, 1995.

58. M.L. KNOTHE TATE, R. STECK, M.R. FORWOOD, P. NIEDERER, In vivo demonstration of load-induced fluid flow in the rat tibia and its potential implications for processes associated with functional adaptation, *J. Exp. Biol.*, Vol.203.19, pp.2737-2745, 2000.

59. J.J. KONIKOFF, Origin of the osseous bioelectric potentials, *Ann. Clin. Lab. Sci.*, Vol.5, pp.330-337, 1975.

60. C.M. KORSTJENS, W.G.M. GERAETS, F.C. VAN GINKEL, B. PRAHL-ANDERSEN, P.F. VAN DER STELT, E.H. BURGER, Longitudinal analysis of radiographic trabecular pattern by image processing, *Bone*, Vol.17, pp.527-532, 1995.

61. L.E. LANYON, Osteocytes, strain detection, bone modeling and remodeling, *Calcified Tissue International*, Vol.53, Suppl. 1, pp.102-106, 1993.

62. A. LEBLANC, V. SCHNEIDER, E. SPECTOR, H. EVANS, R. ROWE, H. LANE, L. DEMERS, A. LIPTON, Calcium absorption, endogenous excretion, and endocrine changes during and after long-term bed rest, *Bone*, Vol.16, pp.301-304, 1995.

63. M. LISKOVA, J. HERT, Reaction of bone to mechanical stimuli. Part 2. Periosteal and endosteal reaction to tibial diaphysis in rabbit to intermittent loading, *Folia Morphol.*, Vol.19, pp.301-317, 1971.

64. G. LUO, S.C. COWIN, A.M. SADEGH, Y.P. ARRAMON, Implementation of strain rate as a bone remodeling stimulus, *J. Biomech. Engr.*, Vol.117, pp.329-338, 1995.

65. S. MORI, R. HARRUFF, W. AMBROSIUS, D. B. BURR, Trabecular bone volume and microdamage accumulation in the femoral heads of women with and without femoral neck fractures, *Bone*, Vol.21, pp.521-526, 1997.

66. C. MATTHECK, Design in Nature, *Springer-Verlag*, Berlin 1998.

67. J. R. MOSLEY, L. E. LANYON, Strain rate as a controlling influence on adaptive modeling in response to dynamic loading of the ulna in growing male rats, *Bone*, Vol.23, pp.313-318, 1998.

68. M.G. MULLENDER, R. HUISKES, A proposal for the regulatory mechanism of Wolff's Law, *J. Orthop. Res.*, Vol.13, pp.503-512, 1995.

69. M.G. MULLENDER, R. HUISKES, Osteocyte and bone lining cells – which are the best candidates for mechano-sensors in cancellous bone?, *Bone*, Vol.6, pp.527-532, 1997.

70. M.G. MULLENDER, R. HUISKES, H. WEINANS, A physiological approach to the simulation of bone remodeling as a self-organizational control process (Technical Note), *J. Biomech.*, Vol.27, pp.1389-1394, 1994.

71. M.G. MULLENDER, R. HUISKES, H. VERSLEYEN, P. BUMA, Osteocyte density and histomorphometric parameters in cancellous bone of the proximal femur in five mammalian species, *J. Orthop. Res.*, Vol.14, pp.972-979, 1996.

72. M.G. MULLENDER, R. HUISKES, B. VAN RIETBERGEN, P. RUEGSEGGER, Effect of mechanical set-point of bone cells on mechanical control of trabecular bone architecture, *Bone*, Vol.22, pp.125-131, 1998.

73. M.G. MULLENDER, R. HUISKES, D.D. VAN DER MEER, P. LIPS, Osteocyte density changes in aging and osteoporosis, *Bone*, Vol.18, pp.109-113, 1996a.

74. M.G. MULLENDER, R. HUISKES, H. VERSLYEN , P. BUMA, Osteocyte density and histomorphometric parameters in cancellous bone of the proximal femur in five mammalian species, *Journal of Orthopaedic Research*, Vol.14, pp.972-979, 1996b.

75. A. NAFEI, C.C. DANIELSEN, F. LINDE, I. HVID, Properties of growing trabecular ovine bone. Part I: mechanical and physical properties, *J. Bone Joint. Surg. [Br]*, Vol.82B, pp.910-920, 2000a.

76. A. NAFEI, J. KABEL, A. ODGAARD, F. LINDE, I. HVID, Properties of growing trabecular ovine bone. Part II: architectural and mechanical properties, *J. Bone Joint. Surg. [Br]*, Vol.82B, pp.921-927, 2000b.

77. B. S. NOBLE, H. STEVENS, J. REEVE, N. LOVERIDGE, Identification of apoptotic changes in osteocytes in normal and pathological human bone, *Bone*, Vol.20, pp.273-282, 1997.

78. A.M. PARFITT, R. TRAVERS, F. RAUCH, F.H. GLORIEUX, Structural and cellular changes during bone growth in healthy children, *Bone*, Vol.27, pp.487-494, 2000.

79. F. PAUWELS, Biomechanics of fracture healing, *Biomechanics of the Locomotor Apparatus (Translated from the 1965 German edition by P. Manquet and R. Furlong)*, pp.106-120, Springer, Berlin, 1980.

80. U. E. PAZZAGLIA, L. ANDRINI, A. DI NUCCI, The effects of mechanical forces on bones and joints, *J. Bone Jt. Surg.* , Vol.79-B, pp.1025-1030, 1997.

81. D. PIENKOWSKI , S.R. POLLACK, The origin of stress-generated potentials in fluid-saturated bone, *J. Orthop. Res.*, Vol.1, pp.30-41, 1983.

82. P.J. PRENDERGAST, D. TAYLOR, Prediction of bone adaptation using damage accumulation, *J. Biomechanics*, Vol.27, pp.1067-1076, 1994.

83. G. A. RODAN, Mechanical loading, estrogen deficiency, and the coupling of bone formation to bone resorption, *J. Bone Min. Res.*, Vol.6, pp.527-530, 1991.

84. H. ROESLER, The history of some fundamental concepts in bone biomechanics, *J. Biomech.*, Vol.20, pp.1025-1034, 1987.

85. W. ROUX, Der züchtende Kampf der Teile, oder die 'Teilauslese' im Organismus , *Theorie der 'funktionellen Anpassung'*, Wilhelm Engelman, Leipzig, 1881.

86. C. T. RUBIN, L. E. LANYON, Osteoregulatory nature of mechanical stimuli: function as a determinant for adaptive bone remodeling, *J. Orthop. Res.*, Vol.5, pp.300-310, 1987.

87. R. RUIMERMAN, R. HUISKES, H. VAN LENTHE, J.D. JANSSEN, A computer-simulation model relating bone- cell metabolism to mechanical adaptation of trabecular architecture, *Comp. Meth. in Biom. and Bioeng.*, Vol.4, pp.433-448, 2001.

88. T.M. SKERRY, L. BITENSKY, J. CHAYEN, L.E. LANYON, Early strain-related changes in enzyme activity in osteocytes following bone loading in vivo, *J. Bone Min. Res.*, Vol.4, pp.783-788, 1989.

89. TH. S. SMIT, E. H. BURGER, Is BMU-coupling a strain-regulated phenomenon?, *J. Bone Min. Res.*, Vol.15, pp.301-307, 2000.

90. W. SONTAG, Age-dependent morphometric alterations in the distal femora of male and female rats, *Bone*, Vol.13, pp.297-310, 1992.

91. I. STEWART, *Life's Other Secret*, Allen Lane/The Penguin Press, London, 1992.

92. E. TANCK, L. BLANKEVOORT, A. HAAIJMAN, E.H. BURGER, R. HUISKES, The influence of muscular activity on local mineralization patterns in metatarsals of the embryonic mouse, *J. Orthop. Res.*, Vol.18, pp.613-619, 2000.

93. E. TANCK, J. HOMMINGA, H.G. VAN LENTHE, R. HUISKES, Increase in bone volume fraction precedes architectural adaptation in growing bone, *Bone*, Vol.28, pp.650-654, 2001.

94. C.H. TURNER, Three rules for bone adaptation to mechanical stimuli, *Bone*, Vol.23, pp.399-497, 1998.

95. C.H. TURNER, I. OWAN, Y. TAKANO, Mechanotransduction in bone: role of strain rate, *Am. J. Physiol.*, Vol.269, pp.438-442, 1995.

96. N. UDAGAWA, Osteoblasts/stromal cells stimulate osteoclast activation through expression of osteoclast differentiation factor/RANKL but not macrophage colony-stimulating factor, *Bone*, Vol.25, pp.517-523, 1999.

97. H. VAN LENTHE, M. DE WAAL MALEFIJT, R. HUISKES, Bone resorption in the distal femur after total knee arthroplasty can be caused by stress shielding, *J. Bone Jt. Surg.*, Vol.79B, 117-122, 1999.

98. J.W.A. VAN LOON, D.J. BERVOETS, E.H. BURGER, S.C. DIEUDONNÉ, J.W. HAGEN, C.M. SEMEINS, B. ZANDIEH DOULABI, J.P. VELDHUIJZEN, Decreased mineralization and increased calcium release in isolated fetal mouse long bones under near weightlessness, *J. Bone Miner. Res.*, Vol.10, pp.550-557, 1995.

99. M.C.H. VAN DER MEULEN, G.S. BEAUPRÉ, D.R. CARTER, Mechanobiologic influences in long bone cross- sectional growth, *Bone*, Vol.14, pp.635-642, 1993.

100. B. VAN RIETBERGEN, R. HUISKES, H. WEINANS, D.R. SUMNER, T.M. TURNER, J.O. GALANTE, The mechanism of bone remodeling and resorption around press-fitted THA stems, *J. Biomech.*, Vol.26, pp.369-382, 1993.

101. B. VAN RIETBERGEN, R. HUISKES, M. MULLENDER, Differentiation to plate-like or strut-like architectures in trabecular bone as a result of mechanical loading, *Transactions 41th ORS*, pp.179, 1995.

102. B. VAN RIETBERGEN, R. HUISKES, R. MÜLLER, D. ULRICH, P. RÜEGSEGGER, Tissue stress and strain in trabeculae of a canine proximal femur can be quantified from computer reconstructions, *J. Biomech.*, Vol.32, pp.443-451, 1999.

103. D. VASHISHTH, O. VERBORGT, G. DIVINE, M.B. SCHAFFLER, D.P. FYHRIE, Decline in osteocyte lacunar density in human cortical bone is associated with accumulation of microcracks with age, *Bone*, Vol.26, pp.375-380, 2000.

104. O. VERBORGT, G.J. GIBSON, M.B. SCHAFFLER, Loss of osteocyte integrity in association with microdamage and bone remodeling after fatigue in vivo, *J. Bone Min. Res.*, Vol.15, pp.60-70, 2000.

105. H. WEINANS, R.HUISKES, H.J. GROOTENBOER, The behavior of adaptive bone-remodeling simulation models, *J. Biomech.*, Vol.25, pp.1425-1441, 1992a.

106. H. WEINANS, R.HUISKES, H.J. GROOTENBOER, Effects of material properties of femoral hip components on bone remodeling and interface stresses, *J. Orthop. Res.*, Vol.10, pp.845-853, 1992b.

107. H. WEINANS, R.HUISKES, B. VAN RIETBERGEN, D.R. SUMNER, T.M. TURNER, J.O. GALANTE, Adaptative bone remodeling around bonded noncemented THA: a comparison between animal experiments and computer simulations, *J. Orthop. Res.*, Vol.11, pp.500-513, 1993.

108. S. WEINBAUM, S.C. COWIN, Y. ZENG, A model for the excitation of osteocytes by mechanical loading-induced bone fluid shear stresses, *J. Biomech.*, Vol.27, pp.339-360, 1994.

109. J. WOLFF, The Law of Bone Remodeling, *(Das Gesetz der Transformation der Knochen, Kirchwald, 1892)*, Translated by Maquet, P. and Furlong, R. Springer-Verlag, Berlin, 1986.

110. L. YOU, S.C. COWIN, M.B. SCHAFFLER, S. WEINBAUM, A model for strain amplification in the actin cytoskeleton of osteocytes due to fluid drag on pericellular matrix, *J. Biomech.*, Vol.34, pp.1375-1386, 2001.

111. J.E. ZERWEKH, L. A. RUML, F. GOTTSCHALK, C. Y. C. PAK, The effects of twelve weeks of bed rest on bone histology, biochemical markers of bone turnover, and calcium homeostasis in eleven normal subjects, *J. Bone Min. Res.*, Vol.13, pp.1594-1601, 1998.